



Ice nucleation by water-soluble macromolecules

B. G. Pummer¹, C. Budke², S. Augustin-Bauditz³, D. Niedermeier^{3,4}, L. Felgitsch⁵, C. J. Kampf¹, R. G. Huber⁶, K. R. Liedl⁶, T. Loerting⁷, T. Moschen⁸, M. Schauperl⁶, M. Tollinger⁸, C. E. Morris⁹, H. Wex³, H. Grothe⁵, U. Pöschl¹, T. Koop², and J. Fröhlich-Nowoisky¹

¹Dept. Multiphase Chemistry, Max Planck Institute for Chemistry, Hahn-Meitner-Weg 1, 55128 Mainz, Germany

²Faculty of Chemistry, Bielefeld University, Universitätsstraße 25, 33615 Bielefeld, Germany

³Experimental Aerosol and Cloud Microphysics Dept., Leibniz Institute of Tropospheric Research, Permoserstraße 15, 04318 Leipzig, Germany

⁴Dept. of Physics, Michigan Technological University, 1400 Townsend Drive, 49931 Houghton, Michigan, USA

⁵Inst. for Materials Chemistry, Vienna University of Technology, Getreidemarkt 9, 1060 Vienna, Austria

⁶Inst. for General, Inorganic and Theoretical Chemistry, University of Innsbruck, Innrain 80–82, 6020 Innsbruck, Austria

⁷Inst. for Physical Chemistry, University of Innsbruck, Innrain 80–82, 6020 Innsbruck, Austria

⁸Inst. for Organic Chemistry, Center for Molecular Biosciences Innsbruck, University of Innsbruck, Innrain 80-82, 6020 Innsbruck, Austria

⁹UR0407 Pathologie Végétale, Institut National de la Recherche Agronomique, 84143 Montfavex CEDEX, France

Correspondence to: B. G. Pummer (b.pummer@mpic.de)

Received: 26 August 2014 – Published in Atmos. Chem. Phys. Discuss.: 19 September 2014

Revised: 23 March 2015 – Accepted: 29 March 2015 – Published: 21 April 2015

Abstract. Cloud glaciation is critically important for the global radiation budget (albedo) and for initiation of precipitation. But the freezing of pure water droplets requires cooling to temperatures as low as 235 K. Freezing at higher temperatures requires the presence of an ice nucleator, which serves as a template for arranging water molecules in an ice-like manner. It is often assumed that these ice nucleators have to be insoluble particles. We point out that also free macromolecules which are dissolved in water can efficiently induce ice nucleation: the size of such ice nucleating macromolecules (INMs) is in the range of nanometers, corresponding to the size of the critical ice embryo. As the latter is temperature-dependent, we see a correlation between the size of INMs and the ice nucleation temperature as predicted by classical nucleation theory. Different types of INMs have been found in a wide range of biological species and comprise a variety of chemical structures including proteins, saccharides, and lipids. Our investigation of the fungal species *Acremonium implicatum*, *Isaria farinosa*, and *Mortierella alpina* shows that their ice nucleation activity is caused by proteinaceous water-soluble INMs. We combine these new results and literature data on INMs from fungi, bacteria, and pollen with theoretical calculations to develop a chemical in-

terpretation of ice nucleation and water-soluble INMs. This has atmospheric implications since many of these INMs can be released by fragmentation of the carrier cell and subsequently may be distributed independently. Up to now, this process has not been accounted for in atmospheric models.

1 Introduction

Although ice is thermodynamically favored over liquid water at temperatures below 273.15 K, the phase transition is kinetically hindered. Consequently, supercooled droplets of ultrapure water stay liquid until temperatures as low as 235 K are reached. The spontaneous self-assembling of water molecules in an ice-like arrangement, which is necessary for freezing to occur, is called homogeneous ice nucleation (Fig. 1a). At higher temperatures, catalytic surfaces which act as an ice-mimicking template are necessary. The process, in which water molecules are stabilized in an ice-like arrangement by an impurity, is called heterogeneous ice nucleation (Fig. 1b, c). An impurity that possesses this ability is called an ice nucleator (IN), or sometimes an ice nucleus. The driving force that causes ice nucleation activity (INA)

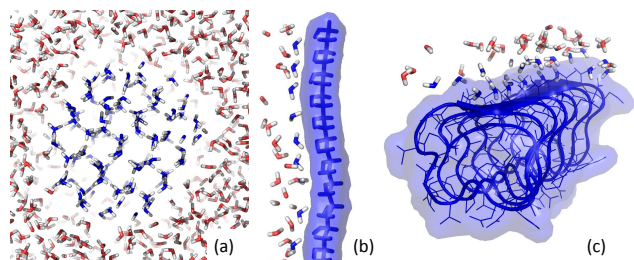


Figure 1. Visualization of water molecule ordering based on molecular model calculations (Sect. S2.1): homogeneous ice nucleation (a); heterogeneous ice nucleation by ordering of water molecules on a polyvinyl alcohol (PVA) strain, which is a 1-D template (b), and an antifreeze protein that has a similar sequence and structure as the bacterial INMs, which is a 2-D template (c). Each image contains water molecules that are ordered (blue) and some randomly distributed water molecules (red).

is the interaction between the partial charges on the H and O atoms in the water molecules and the properly arranged (partial) charges on the IN surface. Therefore, the IN has to carry functional groups at the proper position to be effective (Liou et al., 2000; Zachariassen and Kristiansen, 2000). In most cases it is not the whole surface of an IN that participates in ice nucleation, but only certain sections, which are known as “active sites” (Edwards et al., 1962; Katz, 1962).

The larger the active site of an IN is and the better the functional groups it carries fit the ice lattice, the more effective it stabilizes ice clusters, and so the higher the freezing temperature. Consequently, single molecules with a low molar mass are not well suited to nucleate ice. In fact, soluble compounds consisting of ions, such as salts, or very small molecules, such as sugars and short-chained alcohols, cause a depression of the thermodynamic freezing point and the homogeneous ice nucleation temperature (Koop, 2004). However, if single molecules are so large that they allocate a large enough active surface, they can become INs by themselves. Such ice nucleating macromolecules (INMs) are especially common among biological INs. More information about INMs is given in Sect. S1.1 in the Supplement. For the same reason, some compounds with low molar mass which show no INA in solution can act as INs if they are crystallized in layers of a certain arrangement (Fukuta, 1966). Further information related to the ice nucleation process is compiled in the Supplement (Sects. S1.2, S1.3, and S1.4). INA has been discovered in various forms of life, including certain bacteria, fungi, algae, plants, and animals. Studies for characterizing the active sites of some of these organisms have revealed that they are biopolymers in almost all cases examined. The chemistry of these INMs is as diverse as the range of species they represent (Table 1, Sect. 4.1): overall, proteins, higher saccharides and lipids, and hybrid compounds can play a role in INA, both as singular molecules as well as in aggregated form. They occur in several species of bacteria, fungi, plants,

and animals. Apart from being INMs, they are very diverse in their properties, like size or heat tolerance, as their diverse chemical nature suggests.

In this study, we chemically characterize the water-soluble INMs found in the fungal species *Acremonium implicatum* and *Isaria farinosa* and we compare the results with other recent studies of water-soluble INMs from the fungus *Mortierella alpina* (Fröhlich-Nowoisky et al., 2015), from birch pollen (Pummer et al., 2012; Augustin et al., 2013), and from bacteria (Niedermeier et al., 2014). We also discuss relevant key findings of related earlier studies on the INA of biological materials (e.g., Govindarajan and Lindow, 1988a). Combining these data with calculations derived from classical nucleation theory (Zobrist et al., 2007), we draw conclusions about the nature, sources, and potential atmospheric effects of biological INMs.

2 Methods

2.1 Characterization of new fungal INMs

The fungi *A. implicatum* and *I. farinosa* were cultivated on plates of potato dextrose agar (VWR™), incubated at ambient temperature for 1–2 weeks, until the first mycelium was formed, and then left to grow at ~ 280 K for 2–3 months (*A. implicatum*) or 6–10 months (*I. farinosa*). The mycelium was scratched off with either a scalpel or an inoculating loop and put into a 15 mL Falcon tube. High-purity water ($18.2\text{ M}\Omega \times \text{cm}$) was drawn from a water purification system (Thermo Scientific™ Barnstead GenPure xCAD plus), autoclaved at 394 K for 20 min, and filtrated through a sterile $0.1\ \mu\text{m}$ PES filter (Corning™). Then, 10 mL of the high-purity water was added to the mycelium in the tube, which was then shaken with a vortex device (VWR™ lab dancer) three times for 30 seconds and filtrated through a $5\ \mu\text{m}$ PES syringe filter (Acrodisc®), yielding a transparent solution. A small aliquot of the $5\ \mu\text{m}$ filtrate was branched off for INA measurement as described later in this section, while the rest was further filtrated through a $0.1\ \mu\text{m}$ PES syringe filter (Acrodisc®). A small aliquot of the $0.1\ \mu\text{m}$ filtrate was saved for INA tests. Further aliquots were exposed to different procedures, which are listed below, and then tested for changes in their INA. This provides information about the chemistry of the INMs. In all cases, not only the filtrates but also pure water samples which were treated the same way were tested as a negative reference.

- Filtration through size exclusion filtration tubes (Vivaspin® 500) with a cutoff of 300 and 100 kDa. The passage through a filter indicates that the molecules are smaller than the given cutoff.
- Exposure to heat for 1 h: 308 and 333 K, providing information about thermal stability.

Table 1. Chemical properties of some INs. T_{dn} shows the temperature above which they are denatured. A question mark indicates uncertainty. See Sect. 4.1 for the sources of these data. $\theta[^\circ] \pm \sigma[^\circ]$ are the calculated contact angle distribution according to the soccer ball model.

Type	Organism	Cell-free	Protein	Saccharide	Lipid	T_{dn}	size (1 unit)	$\theta(^\circ) \pm \sigma(^\circ)$
BINMs	<i>P. syringae</i>	–	+	+	+	< 313 K	150–180 kDa	34.1 ± 2.3
	<i>E. herbicola</i>	+	+	+	+	< 313 K	150–180 kDa	
Fungal INs	<i>R. chrysoleuca</i>	+	+	–	–	> 333 K	< 0.22 μm	
	<i>F. avenaceum</i>	+	+	–	–	> 333 K	< 0.22 μm	
	<i>A. implicatum</i>	+	+	–?	+	308–333 K	100–300 kDa	33.2 ± 2.3
	<i>I. farinosa</i>	+	+	–?	–	308–333 K	~ 300 kDa	24.6 ± 0.6
	<i>M. alpina</i>	+	+	–?	–	333–371 K	100–300 kDa	26.4 ± 1.1
	rust spores	??	??	+	??	~ 373 K	??	
Animal INs	<i>Tipula</i>	+	+	+?	+	??	800 kDa	
	<i>Dendroides</i>	+	+	–?	+/-	??	> 70 kDa	
	<i>Vespula</i>	+	+	–	??	< 373 K	74 kDa	
	<i>Eurosta</i> *	+	–	–	–	??	> 100 μm	
Plant INs	<i>Secale</i> leaves	??	+	+	+	< 363 K	??	
	<i>Prunus</i> wood	–	–	??	??	313–323 K	??	
	<i>Betula</i> pollen	+	–	+	–	445–460 K	100–300 kDa	58.2 ± 4.6
	<i>Lobelia</i> fluid	+	–	+?	–	> 373 K	??	
	<i>Opuntia</i> fluid	+	–	+	–	??	< 70 μm	
	different algae	??	??	??	??	??	??	

* Only the calcium phosphate spherules are regarded here, not the fat cells.

- Addition of 6.0 M guanidinium chloride (Promega®), which is a chaotropic reagent used for protein denaturation.
- Addition of 0.3 M boric acid (National Diagnostics®), which esterifies with saccharide OH groups and thereby blocks the site.
- Digestion with enzymes (Applichem®) for at a given incubation temperature: lipase for 1 h at 308 K for fat digestion, papain for 5 h at 296 K for protein digestion. For the latter, two more temperatures were investigated (5 h at 308 K, 1 h at 333 K) since its optimum temperature is about 338 K, but the investigated INMs turned out to be rather thermolabile. Conveniently, papain still functions at temperatures far lower than its optimum, but with lower reaction rates. In our case, the lowest investigated temperature was sufficient.

To determine the IN concentration per gram of mycelium, the same setup and procedure as in Fröhlich-Nowoisky et al. (2015) were applied: each sample was diluted with ultrapure water to an INM concentration where Eq. (1) gives finite results (the proper dilution was determined by trial and error). Then, 50 μL aliquots of the dilute were pipetted into 24–32 wells of a 96-well PCR tray (Axon™), which was sealed with adhesive foil. The plate was inserted into an isolated PCR-plate thermal block, which was tempered by a cooling bath (Julabo™Presto A30). For recording nucleation spectrums, the block was cooled to an initial tem-

perature of 269.15 or 270.15 K. Then, the block was further cooled in 0.5 to 2 K steps each 12 min. After each step, the number of frozen droplets was counted. They can be distinguished from liquid droplets since they reflect incident light differently, and therefore appear much darker. We calculated the IN concentration (number of INs per grams of mycelium) using a variant of the Vali formula (Eq. 1) (Vali, 1971):

$$n_m [g^{-1}] = -\ln(1 - f_{\text{ice}}) \times \frac{V_{\text{wash}}}{V_{\text{drop}}} \times \frac{F_{\text{dil}}}{m_{\text{myc}}}. \quad (1)$$

n_m is the number of INMs per gram of mycelium, f_{ice} the fraction of frozen droplets, V_{wash} the volume of water added for washing (10 mL in this study), V_{drop} the droplet volume in the freezing assay (0.05 mL in this study), F_{dil} the dilution factor of the extract, and m_{myc} the mass of the mycelium. For the formula to work, a proper dilution, where $0 < f_{\text{ice}} < 1$ is fulfilled, is necessary. In the case of $f_{\text{ice}} = 0$, the dilution is too high, and the formula gives $n_m = 0$ as a result. In the case of $f_{\text{ice}} = 1$, the sample is too concentrated since n_m becomes infinite. We note that Eq. (1) assumes that each droplet contains the same number of IN, i.e., the mean number of IN. However, at very small concentrations, the distribution of INMs in the droplets follows Poisson statistics, so that even for a mean number of one INM per droplet, some droplets may contain two or more INMs, and others no INMs at all. Without the use of Poisson statistics all of these would be counted as one in the analysis (Augustin et al., 2013).

To quantify the efficacy of the new-found INMs of *A. implicatum* and *I. farinosa* in comparison with others, we used the soccer ball model (SBM; Niedermeier et al., 2011, 2014), which combines classical nucleation theory with the assumption of a contact angle distribution to calculate mean contact angles θ and standard deviations σ from the 0.1 μm filtrate curves. This is done by determining values for θ and σ such that the measured values of f_{ice} are reproduced by the model. The corresponding equation describing the contact angle distribution and the SBM are given explicitly in Niedermeier et al. (2014). Using a mass-to-size conversion table for proteins from Erickson (2009), we estimated the diameter of our INMs to be about 4 nm, which was used for the SBM parameterization. In comparison, we also calculated mean θ and σ of *M. alpina* from comparable filtrates (Fröhlich-Nowoisky et al., 2015), and added literature data for INMs from birch pollen (Augustin et al., 2013) and bacteria (Niedermeier et al., 2014). The concept of contact angles has, in the past, been applied for ice nucleating particles consisting of mineral dust, for which reasonable results were obtained (e.g., Marcolli et al., 2007; Welti et al., 2012). Here we apply it to describe the ice nucleation induced by water-soluble INMs, and we were able to derive contact angle distributions such that all measured data can be reproduced by the SBM. More specifically, a contact angle distribution determined for a sample reproduced all measurements done for that sample, even if different concentrations, different cooling times or completely different measurement approaches, as those described in the following paragraphs, were used.

INA was also measured with two additional experimental techniques. For both setups, 0.1 μm filtrates that were prepared as described at the top of this section were diluted and applied. These two additional methods were included to expand the data to lower temperatures, which was possible due to the smaller droplet sizes these methods examined (Bielefeld Ice Nucleation ARraY (BINARY) droplet volumes are about 1 μL) and to ensure that possible interactions between the examined droplets and the substrates did not influence the results (Leipzig Aerosol Cloud Interaction Simulator (LACIS) examined freely floating droplets). Resulting values for n_m are compared to the n_m derived from the conventional freezing droplet array. Those systems are

- (i) A droplet freezing array termed BINARY, which consists of a 6×6 array of microliter droplets on a hydrophobic glass slide on top of a Peltier cooling stage. A detailed description of the technique, the preparation of droplets, and the data acquisition and evaluation is given in Budke and Koop (2015).
- (ii) A vertical flow tube named LACIS, which is described in detail in Hartmann et al. (2011). Basically, droplets are generated from the filtrate and dried. The residual particles are then size-selected, humidified to form uniform droplets and inserted into the tube, where they are cooled to the temperature of interest. The procedure was

similar to that for the birch pollen washing waters described in Augustin et al. (2013).

2.2 Characterization of birch pollen INMs

To test the hypotheses that birch pollen INMs are polysaccharides and not proteins (Pummer et al., 2012), further procedures for characterization of the birch pollen INMs were carried out. Therefore, birch pollen extracts were prepared by suspending and shaking 10 mg mL^{-1} pollen in ultrapure water for several hours, and then vacuum filtering the suspension through a 0.1 μm PES filter (CorningTM). The aqueous fraction was then exposed to different treatments, and n_m was determined the same way as for the fungi, with 24 or 32 droplets per sample, at 258 or 256 K. In all cases, reference samples without addition of the reagents were measured and defined as 100 % INA. The results are listed in Table 2.

First, boric acid was added to an aliquot of fungal extract to a concentration of 0.75 M. The aliquot was left overnight at room temperature, as boric acid is known to esterify with sugars. This treatment should alter the INA of the birch pollen INMs, in case that saccharides play a role. However, since the esterification process does not necessarily affect all functional groups, the INA might be only partially eliminated. Since the INA assay preparation has a certain statistical uncertainty, minor changes in the INA are difficult to interpret. Therefore, we also investigated untreated birch pollen extracts as a reference. The same procedure was repeated by heating aliquots with and without boric acid to 343 K for 2 h to accelerate the esterification process.

To check if birch pollen INMs are indeed non-proteinaceous, three separate 100 μL aliquots were each mixed with 94 μL of (i) water, (ii) medium without enzyme, (iii) medium with Trypsin, and were incubated for 18 h at 310 K. Additionally, 100 μL water was treated like (iii). Trypsin is an enzyme that breaks down proteins, but demands a certain medium. For each sample an INA assay as described in Sect. 2.1 was run.

In addition, aliquots of the birch pollen extracts digested with Trypsin and medium before and after incubation were forwarded through a size exclusion chromatography (SEC) column, and the different eluted fractions were tested for their INA. Details about the setup and the measurements are presented in Sect. S2.2. With SEC, we checked if the enzymatic treatment changed the mass range of the birch pollen INMs.

2.3 Ice nucleation experiments with bacterial INM peptides

A sample of the 16-amino acid peptide fragment which is the repetitive element in the bacterial INM (BINM) of *Pseudomonas syringae* was investigated for its INA. The peptide with the primary sequence GSTQTAGESSLTAGY was obtained from PSL (Heidelberg, Germany) and purified chromatographically using a HiTrap Desalting column (GE

Table 2. An overview of the investigation of birch pollen extracts. The percentage is the relative number of INs in comparison to the untreated aliquot at a given temperature T (K). Lines labeled with “(ref)” refer to reference measurements under the same conditions with pure water instead of extract.

Treatment	% INA	T (K)
None	100	both
None (ref)	<9	both
Boric acid	15	256
Boric acid (ref)	0	256
343 K	29	256
343 K + boric acid	3	256
Medium	34	258
Medium + Trypsin	30	258
Medium + Trypsin (ref)	13	258

Healthcare) with high-purity water ($18.2 \text{ M}\Omega \times \text{cm}$) from a Milli-Q water purification system (Millipore). The yield of pure peptide was determined using a NanoPhotometer ($\epsilon_0 = 1490 \text{ M}^{-1} \text{ cm}^{-1}$).

We measured peptide solutions with 10, 20, and 30 mg mL^{-1} using the oil immersion cryo-microscopic method, which is described in detail in Pummer et al. (2012). As such we prepared emulsions consisting of 45 % wt aqueous peptide solution and 55 % wt oil (paraffin–lanolin). The frozen fractions of droplets with diameters of 20–50 μm were documented with the software Minisee[®] as a function of temperature.

3 Results

3.1 Experimental characterization of INMs

The results of the chemical characterization of the fungal filtrates are composed in Fig. 2. The quantitative passage through the 0.1 μm pore size filters, yielding optically transparent, particle-free filtrates, demonstrates that those INMs are cell-free and stay in solution when they are extracted with water.

The initial freezing temperature was 269 K for *I. farinosa* and 264 K for *A. implicatum*. The calculated contact angles for *I. farinosa* and *M. alpina* are the highest, while the one of *A. implicatum* lies in the range of that of the BINM (Table 1). The reduction of INA by papain and by guanidinium chloride indicates that the INMs of both species are proteinaceous. Lipids seem to play a role in *A. implicatum*, but none in *I. farinosa*. Both were resistant against boric acids, making contributions of carbohydrates to the INA unlikely. Both INMs are more heat sensitive than other fungal INMs since they were destroyed at 333 K. *A. implicatum* has a mass of approximately 100 to 300 kDa since it quantitatively passes through the 300 kDa filter, but not through the 100 kDa filter. About 95 % of *I. farinosa* INM were retained in the 300 kDa

filter in comparison to the 0.1 μm filter, and the initial freezing temperature is shifted below 268 K. This suggests that there are larger, more active states of *I. farinosa* INMs and smaller ones active at lower temperatures.

Figure 3 shows the comparison between the data from BINARY, LACIS, and the droplet freezing array (Sect. 2.1). Each strain shows a relatively good overlap of the plateaus obtained with the different methods. Only when comparing the C-strain measurements can a difference in total n_m be seen, which, however, is less than 1 order of magnitude. The initial freezing temperatures are higher for the conventional droplet freezing array in Mainz in comparison with BINARY. This may indicate that the investigated INMs show a small time-dependence, which would lead to an increase in n_m at lower temperature for the experiment with the larger cooling rate (i.e., BINARY), in agreement with the observations. From that it becomes evident that onset temperatures, which were often reported in the past, do not properly describe the ice nucleation process. They depend on the detection limit of the measurement method, as well as the INM content per droplet, and they are influenced by impurities or statistical outliers. Hence, the temperature at which 50 % of all droplets froze (T_{50}) was taken for examination. If we assume that the mass of a single INM is about $100 \text{ kDa} = 1.7 \times 10^{-19}$ grams and that the maximum number density we found was $n_m = 10^{10}$ per gram (Fig. 3), the INMs amount to approximately 1.7 ppb of the total mycelium mass.

The results of the birch pollen measurements, which are given in Table 2, suggest that both the medium for the Trypsin test and the boric acid led to a reduction in INA. The addition of Trypsin had no additional effect, which speaks against the proteinaceous nature of those INMs. It is most likely that it is the formic acid from the medium that decreases the INA in the respective measurement since it esterifies with hydroxyls similar to the boric acid. This is consistent with the resistance against other proteases and guanidinium chloride (Pummer et al., 2012), and the lack of the spectroscopic signature typical for proteins in the most active eluates. Overall, we confirm that the birch pollen INMs are not proteins but most likely polysaccharides. After the elution from the SEC column, small amounts of INMs were spread across all fractions of the eluate. This might be caused by the adhesion of the organic matter in the extracts to the column packing, which undermines the separation principle. The tendency for adhesion of organic matter from pollen was investigated by Pummer et al. (2013b). Nevertheless, there was an unambiguous maximum in the 335 to 860 kDa fraction before and after digestion. In parallel, we recorded the absorbance of the eluate at 280 nm using a UV detector, which is a quite reliable way to detect most proteins. However, the detector showed no signal when the INA maximum was eluted. This alone makes it very unlikely that the birch pollen INMs are proteinaceous. The discrepancy with the mass range stated in Pummer et al. (2012) could be explained by the slightly higher investigation temperatures, which was

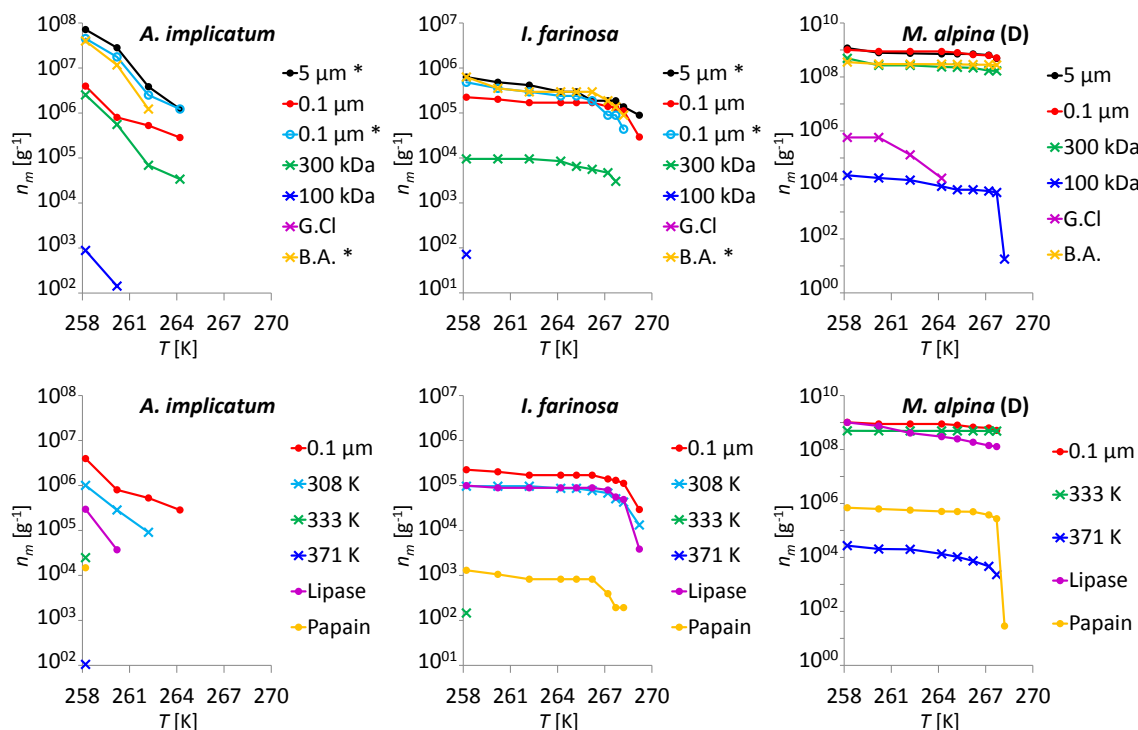


Figure 2. $n_m(T)$ -curves for *A. implicatum*, *I. farinosa*, and *M. alpina* (subgroup D) INMs after different treatments. G.Cl stands for guanidinium chloride treatment, and B.A. for boric acid treatment. A reduction of n_m suggests that this method partly or fully destroyed the INMs. The absence of data points despite the listing in the figure legend indicates that n_m lied below the detection limit. For *M. alpina*, the data are the mean curves of all investigated strains of the phylogenetic subgroup D, which is the most representative (Fröhlich-Nowoisky et al., 2015). The * symbol for *A. implicatum* and *I. farinosa* values: these measurements were undertaken with the filtrates of another harvest, which explains the higher values in comparison to the other results.

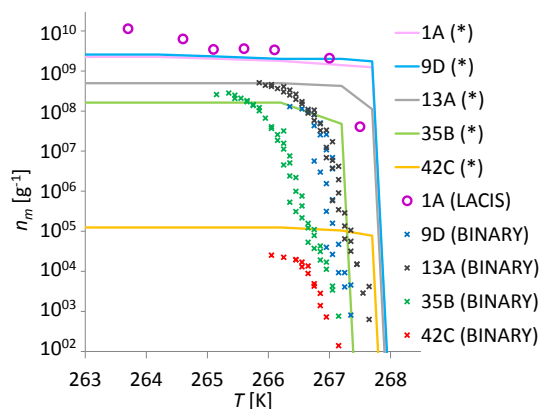


Figure 3. Comparison of ice nucleation curves of 0.1 μm filtrates from a few *M. alpina* strains. The number and letter combination labels the strain. The devices used for generating the respective curves are shown in brackets. * stands for the setup described in Fröhlich-Nowoisky et al. (2015).

a necessity of the setup, which corresponds to a larger critical ice embryo or INM size. We suggest that the birch pollen INMs might be capable of forming aggregates that are larger,

active at higher temperatures, but also less frequent. Consequently, they are below the detection limit of INA assay devices with lower material loads per droplet, such as the oil immersion cryo-microscopy.

The examination shows that the 16-amino acid BINM peptide shows INA when a certain concentration in solution is surpassed. This molecule should hardly show INA since its molecular mass is only 1.6 kDa and the number of fitting functional groups is limited to one TXT motif, where T designates threonine and X any other amino acid. However, these peptides tend to self-assemble into aggregates (Garham et al., 2011), which consequently follow an equilibrium of formation and decay. These aggregates may have different sizes and shapes, and consequently different INAs.

The 10 mg mL⁻¹ sample showed only homogeneous ice nucleation. The 30 mg mL⁻¹ sample showed an initial freezing temperature at about 250 K, a flat slope of $n_m(T)$ towards lower temperatures, and a T_{50} between 240 and 245 K in different experiments. The variance is rather high since the aggregate formation seems to be very sensitive to the handling of the sample. This is in contrast to the typical biological INMs, which show a very steep slope at a given temperature and then reach a saturation plateau (e.g., Figs. 2 and 3). Fur-

ther investigations are in progress to measure the aggregates and get a better understanding of the process.

3.2 Comparison with theoretical calculations of the critical ice embryo size

In Fig. 4, we plot the experimentally determined molecular masses of INMs against the observed ice nucleation temperature. For comparison, we show the theoretical parameterization of the critical ice embryo size of Zobrist et al. (2007), which is based on classical nucleation theory. The sources of the plotted data are specified in Table 3. Apart from the fungal and birch pollen INMs investigated in our groups, we added BINM data from Govindarajan and Lindow (1988a), who indicated the good agreement between aggregate size and critical ice embryo size. INA data of polyvinyl alcohol (PVA) were incorporated since it also showed a slight INA in experiments (Ogawa et al., 2009). Its peculiarities are first that the formula is quite simple for a macromolecule, which is a sequence of CH_2CHOH units, and second, that the chain is rather randomly coiled. Therefore, the near-range molecular order is quite well defined, while the far-range order is merely statistical.

The data of birch pollen and fungal INMs are in acceptable agreement with the theoretical parameterization. We deduce that these free biological INMs which carry a suitable hydration shell mimic a theoretical ice embryo of the same size well enough to show the same INA. However, ice embryos of this size are almost impossible to form spontaneously, which explains the low temperatures that are necessary for homogeneous ice nucleation. In contrast, the biological INMs have a given shape, which explains their high INA.

In the case of PVA, we see that an increase in size does not lead to an appropriate increase in the freezing temperature. This can be easily explained by the different degrees of structure of biological macromolecules and technical homopolymers. Both PVA and BINMs consist of a sequence of monomers covalently linked to each other. Longer chains fold into compact three-dimensional structures. Without any further forces, polymers coil randomly. Therefore, confined geometries do not exceed the size of a few monomers, where the limited flexibility of the monomer-to-monomer bond enforces certain geometries. Hence, an increase in the total INM mass will not increase its INA. In contrast, intact proteins show strongly determined folding, which is held together by intramolecular forces, and sometimes even forced onto them by folding-supporting proteins. Therefore, a native protein's structure is stabilized in a certain geometry as is the molecular surface. The unfolding of a biological macromolecule – a process called denaturation – changes many of its properties. This is also valid for the INA of INMs, and explains their deactivation from heat far below the temperatures where the covalent molecular bonds are broken. It is also responsible for the destruction of most INMs by the chaotropic guanidinium chloride. Summed up, randomly coiled INMs

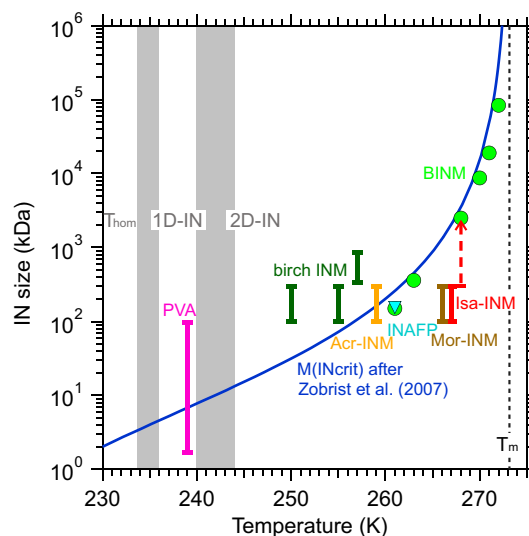


Figure 4. The dependence of the median freezing temperature on size for different types of IN (colored dots). The blue curve is the calculated critical ice cluster size derived from classical nucleation theory (Zobrist et al., 2007). The sources of the presented IN data are listed in Table 3. The graph further shows the region where we assume the domains where 1-D and 2-D templates act as IN. The grey areas mark the transition regions between the domains. The acronyms *Acr*, *Isa*, and *Mor* stand for the respective fungal species.

like PVA allocate only small, one-dimensional templates for ice nucleation (Fig. 1b) and therefore nucleate ice at very low temperatures (Fig. 4). On the other hand, molecules in long-range confined geometries, like the BINM, allocate stable two-dimensional surfaces as ice nucleating templates (Fig. 1c), which are larger and therefore nucleate at higher temperatures (Fig. 4). Also, long-chained alcohols show appreciable INA if they are crystallized in well-defined monolayers, depending on the chain length, the position of the OH group, and substitutions on the side chains (Popovitz-Biro et al., 1994).

4 Discussion

4.1 Previous findings on biological INMs

The previously mentioned BINMs that have been found so far are a certain class of bacterial lipoglycoproteins that are fully sequenced and characterized (e.g., Abe et al., 1989). In some cases, biological INMs of one type or species show more than one freezing temperature on an ice nucleation spectrum. This variation in INA can be explained by the presence of different functional groups, foldings, or aggregation states (e.g., Govindarajan and Lindow, 1988a; Augustin et al., 2013; Dreischmeier et al., 2014; this study). The presence of INMs seems to have certain benefits which lead to their expression in several organisms (Sect. S1.5).

Table 3. Overview over masses (m) and activation temperatures (T_{nuc}) of certain IN.

Type	Source	m (kDa)	T_{nuc} (K)
BINM (~ 560 units)	Burke and Lindow (1990)	~ 83 700	272
BINM (~ 130 units)	Govindarajan and Lindow (1988a)	~ 19 000	271
BINM (~ 60 units)	Govindarajan and Lindow (1988a)	~ 8700	270
BINM (~ 20 units)	Govindarajan and Lindow (1988a)	~ 2500	268
Crit. ice embryo	Zachariassen and Kristiansen (2000)	810	268
<i>Isa</i> -INM (> 1 units)	this study	> 300	268
<i>Isa</i> -INM (1 unit)	this study	100–300	267
<i>Mor</i> -INM	Fröhlich-Nowoisky et al. (2015)	100–300	266
BINM (3 units)	Gurian-Sherman and Lindow (1995)	~ 360	263
BINM (1 unit)	Govindarajan and Lindow (1988a)	~ 150	261
INAFP	Xu et al. (1998)	164	261
<i>Acr</i> -INM	this study	100–300	259
birch INM	this study	335–860	257
birch INM	Pummer et al. (2012)	100–300	255
birch INM*	Augustin et al. (2013)	100–300	250
PVA	Ogawa et al. (2009)	1.7–98	239
Crit. ice embryo	Zachariassen and Kristiansen (2000)	1.26	233

* T_{nuc} here are T_{50} of both the LACIS measurement with 800 nm particles and the oil immersion cryo-microscopy measurement with $5 \mu\text{g mL}^{-1}$ pollen.

The bacterial gene is highly conserved and codes for a 120 kDa β -helical membrane protein with many repeated octapeptides (Green and Warren, 1985; Abe et al., 1989; Kajiya and Lindow, 1993; Schmid et al., 1997; Graether and Jia, 2001; Garnham et al., 2011). The INA induced by this protein also involves glycosides and lipids that stabilize it in the outer membrane of the bacterial cell and assure its conformation for optimum functioning (Kozloff et al., 1984; Govindarajan and Lindow, 1988a; Turner et al., 1991; Kawahara, 2002). With the side chains, the total mass of a single BINM is about 150–180 kDa (Table 1). It is assumed that the initiation point for ice formation is the amino acid sequence TXT in the repeated octapeptide, where T designates threonine and X any other amino acid. The OH groups of the two threonine moieties match the position of oxygen atoms in the ice lattice. Since a BINM contains several of these sequences at positions and distances that correspond to the ice lattice structure, it can stabilize an ice embryo and so decrease the activation barrier for ice nucleation (Graether and Jia, 2001). As sequence modification studies on a structurally related antifreeze protein have shown, the loss of the TXT has a devastating effect on the interaction with water molecules, while other modifications have a much weaker impact (Graether et al., 2000).

The expression of BINMs is an exclusive property of certain bacterial species. It has been reported for a wide range of strains in the *P. syringae* species complex (Lindow et al., 1982; Berge et al., 2014), *P. fluorescens* and *borealis* (Fall and Schnell, 1985; Obata et al., 1987; Foreman et al., 2013), *Erwinia uredovora* (Obata et al., 1990a), *Pantoea agglomerans* (formerly called *E. herbicola*; Phelps et

al., 1986), *Pantoea ananatis* (Coutinho and Venter, 2009), *Xanthomonas campestris* (Kim et al., 1987), a *Pseudoxanthomonas* sp. (Joly et al., 2013), and more. The efficacy of their INA depends on both the strain and the cultural growth conditions, e.g., available nutrients and growth temperature (Rogers et al., 1987; Nemecek-Marshall et al., 1993; Fall and Fall, 1998). In most cases, these BINMs are aggregated and anchored in the outer cell membrane, where the strength of the INA depends on the aggregation state and the chemistry of the membrane (Govindarajan and Lindow, 1988a, b; Kozloff et al., 1991). However, free BINMs still show appreciable INA, although less than in the native state (Schmid et al., 1997). Since these complexes of aggregated BINMs exhibit a large surface that matches the ice crystal lattice almost perfectly, the bacteria expressing them are the most active IN known at present.

These anchored aggregates of BINMs on the otherwise ice nucleation inactive cell surface are a demonstrative example of active sites on a larger IN, which is the micro-sized bacterial cell. In some cases, bacteria release their active sites carried on much smaller membrane vesicles. These are spherical pieces of the outer cellular membrane that are excised from the cell, a natural and common phenomenon in bacteria in general (Deatherage and Cookson, 2012). The expression of such vesicles with BINMs has been reported for *Pantoea agglomerans*/*E. herbicola* (Phelps et al., 1986), *E. uredovora* (Kawahara et al., 1993), and *P. fluorescens* (Obata et al., 1993). *P. syringae* and *viridiflava* express such BINM-carrying vesicles only under certain growth conditions (Obata et al., 1990b; Pooley and Brown, 1990). For *P. putida*, the INA found in culture supernatants was associated

with a 164 kDa lipoglycoprotein and had activity both as an IN and as an antifreeze protein. In this case, removal of the approximately 92 kDa of carbohydrates eliminated the INA but not the antifreeze properties (Xu et al., 1998).

INMs have also been found in the Fungi kingdom (Jayaweera and Flanagan, 1982; Kieft, 1988; Kieft and Ahmadjian, 1989; Kieft and Ruscetti, 1990; Pouleur et al., 1992; Hasegawa et al., 1994; Tsumuki and Konno, 1994; Tsumuki et al., 1995; Richard et al., 1996; Humphreys et al., 2001; Morris et al., 2013; Haga et al., 2014; Fröhlich-Nowoisky et al., 2015). Similarly to the bacteria, only a limited fraction of investigated strains showed INA, while the majority was inactive (Pouleur et al., 1992; Tsumuki et al., 1995; Iannone et al., 2011; Pummer et al., 2013a; Huffman et al., 2013; Fröhlich-Nowoisky et al., 2015). Fungal INMs can be divided into two subgroups, both of which differ from the BINMs. The INMs of rust fungi show properties of polysaccharide compounds (Morris et al., 2013). The previously characterized INMs from *Rhizoplasma chrysosoleuca* (Kieft and Ruscetti, 1990), *F. avenaceum* (Pouleur et al., 1992; Hasegawa et al., 1994; Tsumuki and Konno, 1994), and *M. alpina* (Fröhlich-Nowoisky et al., 2015) are evidently proteins, but show hardly any other similarities with the BINMs. They are more tolerant to stresses, have a different amino acid sequence, seem to have less to no lipid and carbohydrate functionalizing, and are easily released from the cells. Only recently was a 49 kDa protein from *F. acuminatum* suggested as being the INM (Lagzian et al., 2014).

Proteins and lipoproteins with INA were also found in extracellular fluids of insects like *Tipula trivittata* larvae (Duman et al., 1985, 1991; Neven et al., 1989; Warren and Wolber, 1991), *Vespa maculata* queens (Duman et al., 1984), and *Dendroides canadensis* larvae (Olsen and Duman, 1997). The only non-proteinaceous insect INs found up to date are phosphate spherules and fat cells in the larvae of *Eurosta solidaginis* (Mugnano et al., 1996). INs have also been detected in other animal taxa, e.g., amphibians (Wolanczyk et al., 1990) and mollusks (Aunaas, 1982; Hayes and Loomis, 1985; Madison et al., 1991; Lundheim, 1997), as well as in spider silk (Murase et al., 2001).

The fluid reservoirs of some succulent plants, namely *Lobelia telekii* and *Opuntia* species, contain polysaccharide INMs (Krog et al., 1979; Goldstein and Nobel, 1991, 1994). Other reported non-proteinaceous plant INs are from the wood of *Prunus* species (Gross et al., 1988), and the lignin in a waste water sample (Gao et al., 1999). Among plant INs, only those of *Secale cereale* were identified as proteins (Brush et al., 1994). The pollen of some plant species showed appreciable INA in different lab studies, among which that of the silver birch (*Betula pendula* or *alba*) was the most active (Diehl et al., 2001, 2002; von Blohn et al., 2005; Pummer et al., 2012; Augustin et al., 2013). Birch pollen contain easily extractable, very robust INMs, which are non-proteinaceous and most likely some type of polysaccharide (Pummer et al., 2012). The extracts were characterized using vibrational

spectroscopy, which indicated that they contained sugar-like compounds, proteins, and other biological molecules, but no sporopollenin, which is the fabric of the outer pollen wall (Pummer et al., 2013b).

Other organic aerosols which have been the focus of ice nucleation research are humic-like substances (HULIS) and secondary organic aerosols (SOAs). They show certain similarities to the presented INMs since they consist of a large variety of organic macromolecules that have undergone complex biochemical processing. Analogously, several exponents showed little to no INA in experiments, or even oppressed INA in mixed particles by blocking active sites (e.g., Möhler et al., 2008; Prenni et al., 2009), while others showed appreciable INA. Certain HULIS (Wang and Knopf, 2011) and some SOAs (Wang et al., 2012; Schill et al., 2014) induced ice nucleation in the deposition and the immersion mode. The O/C ratio of the latter did not affect the INA, although it influenced several other properties, such as the kinetics of the water uptake, in agreement with recent model simulations (Berkemeier et al., 2014). Among glassy aerosols composed of saccharidic components, some chemical species showed significant INA that might even compete with mineral dust INA in mid-latitude clouds (Wilson et al., 2012). Even a simple compound like citric acid shows INA when it is in the state of a glassy aerosol (Murray et al., 2010). Alternatively, other organic compounds such as oxalic acid can act as an immersion IN in the crystalline state (Zobrist et al., 2006; Wagner et al., 2011). Also, cellulose, which is the most common biopolymer on Earth due to its ubiquity in plant cell walls, shows INA in the form of microcrystalline or fibrous particles (Hiranuma et al., 2015). The inorganic salt ammonium sulfate possesses INA in the crystalline state in both the immersion and deposition mode, despite it being a highly soluble compound (Zuberi et al., 2001; Abbatt et al., 2006).

4.2 Solubility of INMs

In atmospheric science, INs are traditionally regarded as insoluble particles on the surface of which ice nucleation takes place. According to Raoult's law, soluble substances are expected to decrease the freezing point with increasing molar concentration. Furthermore, any ice nucleating template requires a certain size to be able to support a critical ice embryo that is large enough to grow into a macroscopic crystal. Consequently, particles that dissociate into molecules or ions with low molar mass in solution (e.g., NaCl, and mono- and disaccharides) cannot act as IN. However, data from Pummer et al. (2012) showed that the ice nucleation active components of pollen have a mass between 100 and 300 kDa. This means that the INs have the size of single macromolecules. If these molecules are fully dissolved in water, one can regard them as being in solution and not in suspension. Many proteins are soluble in water (e.g., Osborne, 1910; Macedo, 2005; Sect. S1.1), but single protein

molecules are far larger than e.g., salt ions or low molecular weight saccharides. Therefore, a deviation from the simplistic approach of Raoult's law is expected. In this case, a soluble compound can also act as an IN if the active molecular surface is large enough to stabilize ice embryos of critical size. The freezing point depression is expected to be rather weak for a dissolved > 100 kDa molecule because even a high mass concentration correlates with only a low molar concentration. The resulting small reduction of the solution's water activity is likely to affect the heterogeneous ice nucleation temperature only slightly (Sect. S1.4, Koop and Zobrist, 2009; Attard et al., 2012). Accordingly, certain macromolecules can act as IN in spite of being water-soluble because the water-structuring effect overcompensates for the colligative freezing point depression. Most molecules carry a well-defined hydration shell. In the case of INMs, the geometry of water molecules in the hydration shell is supposedly similar to the geometry in an ice embryo, which triggers the freezing process (Fig. 1). We therefore emphasize that a more molecular view of IN allows for a better understanding of the process of heterogeneous ice nucleation. For example, the contact angle, which is useful in atmospheric models, is a macroscopic interpretation of the affinity between two phases: the ice embryo and the IN. Water molecules show a high affinity towards hydroxy (-OH) and amino (-NH₂) groups since they form hydrogen bonds with them. The contact angle quantifies the outcome of the molecular interaction and allows for the comparison of different INs, but it does not allow one to trace back the complex molecular structures that are responsible. If we understand which structures are the characteristics of INMs, it will make predictions of INA possible for any macromolecule with a known sequence. As an example, the previously mentioned TXT sequences (Sect. 4.1) are one such element that foster INA, but there must be others as well since non-proteinaceous INs exist. Classification and precise characterization of the currently known INs might reveal other INA elements.

As shown in Fig. 4, molecular size and INA exhibit a positive correlation. Deviations from the model line can be explained by different properties of different types of INMs. If molecules are larger than expected, like for birch pollen INMs, the active site might not cover the whole molecule, but just a small part of it. The INMs of *I. farinosa* and *M. alpina* seem to be too small. This can be either explained by spontaneous aggregation of several molecules after the filtration step, or by the ability to form a larger hydration shell, which has to be taken into account. Also, when data were derived from measurements in which droplets were examined which contain higher numbers of INM per droplet, the freezing temperature is shifted to higher temperatures, as can be seen, e.g., when comparing data of birch pollen from Pummer et al. (2012) and Augustin et al. (2013). Very speculatively, one could try to go the other way and use experimentally determined freezing temperatures of IN, e.g., mineral dust and soot, to roughly estimate the size of their active sites.

In combination with chemical and structural analyzing of the IN, one could try to identify which elements of these IN can be considered to be responsible for the INA. Considerations about the INA and active sites of mineral dust are given in Sect. S1.6.

4.3 Potential atmospheric effects

Apart from its cryobiological and evolutionary aspect, heterogeneous ice nucleation is of high importance for atmospheric research since it causes cloud glaciation and therefore impacts the global radiation budget (albedo) and initiates precipitation.

A common argument against the atmospheric INA potential of bioaerosols is that whole cells which are at least some micrometers in size are far too large to reach altitudes higher than a few kilometers. However, the detection of cultivable microorganisms, even in the mesosphere (Imshenetsky et al., 1978), shows that there have to be mechanisms that elevate intact cells to the higher atmosphere despite their size. As an example, the atmospheric turbulence caused by volcanic activity support a high- and far-range distribution of all kinds of aerosols (van Eaton et al., 2013). Furthermore, certain pollen (e.g., pine) and fungal spores (e.g., urediospores) are very buoyant, as they possess wing-like projections and other aerodynamic surface properties. Urediospores have been collected from the air at over 3 km above the ground level along with other microorganisms (Stakman and Christensen, 1946). Cultivable microorganisms are also present in the stratosphere (Griffin, 2004) and in cloud water samples (e.g., Vaitilingom et al., 2012; Joly et al., 2013). Even more intriguingly, some of these organisms are even able to proliferate in supercooled cloud droplets (e.g., Sattler et al., 2001).

Biological cells are not rigid spheres, but rather a composition of many different membranes, organelles, and fluids, which further consist of many different molecules, ranging from water to small organic molecules to biopolymers. Therefore, the release of molecular matter, as well as cell fragmentation, is common. Several studies have detected molecular tracers from pollen grains and fungi in atmospheric fine particulate matter even in the absence of whole cells (e.g., Solomon et al., 1983; Yttri et al., 2007). In most cases, biological INMs are easily released from the producing cell (Table 1). Since a single primary biological particle can carry up to hundreds and thousands of INMs, and since the INMs are also much lighter, we expect their atmospheric concentration to be significantly higher as well. A possible mechanism of INM release is cell rupture caused by a rapid change in moisture. Scanning electron microscopy studies on wet pollen back up this idea by visualizing the release of organelles and organic matter (Grote et al., 2001, 2003; Pummer et al., 2013b). This explains why rainfall, which is expected to wash out aerosols, can indeed increase the concentration of allergens (Schäppi et al., 1997) or INs (Huffman

et al., 2013) in the air. Recently, the presence of nanosized biological particles with INA were detected in precipitation (Santl-Temkiv et al., 2015) and soil (O'Sullivan et al., 2015).

Quantifying the atmospheric impact of fungi is even more difficult as presumably 1 to 5 million fungal species exist (Hawksworth, 2001). Due to mutation and adaptation, every species consists of numerous strains, which differ in their INA (Tsumuki et al., 1995). Even if all studies are combined, it is only a minor fraction of all fungal species that have been tested for their INA. Furthermore, the expression of INMs is triggered by yet unknown conditions, which could be the availability of nutrients, the local climate or competition with other microorganisms. As a consequence, INA-positive strains can lose their activity when they are cultivated under laboratory conditions (Tsumuki et al., 1995; Pummer et al., 2013a). Therefore, more atmospheric IN counting and sampling will be necessary to understand the contribution of biological INA better.

Several former studies have focused on quantifying biological INs either by analyzing precipitation samples (Christner et al., 2008a, b), or by atmospheric modeling based on emission and deposition data (Hoose et al., 2010). In both cases, however, only whole cells were examined. Christner et al. (2008a, b) filtered the particles of interest out of the samples, and so lost the molecular fraction, which contains the INMs we described. Hoose et al. (2010) did not include fragmentation or phase separation processes that can release molecular compounds from the carrier particles in the atmosphere. This might have led to an underestimation of the atmospheric relevance of biological INs.

5 Conclusions

Even free water-soluble macromolecules are able to nucleate ice since they are in the same size range as the critical ice embryos. INMs can be diverse in chemical structure and origin, which may range from biopolymers in primary biological aerosols (proteins, saccharides, lipids, hybrid compounds), to secondary organic aerosol components (HULIS, etc.), to synthetic polymers (PVA).

The allocation of functional groups, as well as the confinement that keeps them in place, is essential for the efficacy of the INMs. An increase of the template size that can be realized by aggregation of single molecules also leads to an enhancement of the INA. In this study we have shown that the water-soluble INMs from the fungal species *A. implicatum* and *I. farinosa* are proteins, and we have obtained additional evidence that the birch pollen INMs are polysaccharides without relevant protein content.

Water-soluble INMs are released by a wide range of biological species. They may be associated not only with primary biological aerosols but also with other atmospheric aerosol particles such as soil dust or sea spray. The potential effects of such INMs should be considered and pose an ad-

ditional challenge to the quantification and assessment of the importance of biological ice nucleation in the atmosphere.

The Supplement related to this article is available online at doi:10.5194/acp-15-4077-2015-supplement.

Acknowledgements. We thank the Max Planck Society and the INUIT Research Unit (projects PO1013/5-1, KO2944/2-1, and WE4722/1-1; all for INUIT 1525) for project funding. We acknowledge M. Linden and D. Sebazungu for technical support, as well as Z. Dráb from Pharmallerga® for the donation of the birch pollen.

D. Niedermeier acknowledges financial support from the Alexander von Humboldt Foundation. H. Grothe and T. Loerting are grateful for support from the Austrian Science Fund (FWF; projects P23027 and P26040). We thank the European Science Foundation for funding the workshops on ice nucleation within the research networking programme MicroDICE in the years 2013, 2014, and 2015.

The article processing charges for this open-access publication were covered by the Max Planck Society.

Edited by: A. Bertram

References

- Abbatt, J. P. D., Benz, S., Cziczo, D. J., Kanji, Z., Lohmann, U., and Möhler, O.: Solid ammonium sulfate aerosols as ice nuclei: a pathway for cirrus cloud formation, *Science*, 22, 313, 1770–1773, doi:10.1126/science.1129726, 2006.
- Abe, K., Watabe, S., Emori, Y., Watanabe, M., and Arai, S.: An ice nucleation gene of *Erwinia ananas*, *FEBS Lett.*, 258, 297–300, doi:10.1016/0014-5793(89)81678-3, 1989.
- Attard, E., Yang, H., Delort, A.-M., Amato, P., Pöschl, U., Glaux, C., Koop, T., and Morris, C. E.: Effects of atmospheric conditions on ice nucleation activity of *Pseudomonas*, *Atmos. Chem. Phys.*, 12, 10667–10677, doi:10.5194/acp-12-10667-2012, 2012.
- Augustin, S., Wex, H., Niedermeier, D., Pummer, B., Grothe, H., Hartmann, S., Tomsche, L., Clauss, T., Voigtländer, J., Ignatius, K., and Stratmann, F.: Immersion freezing of birch pollen washing water, *Atmos. Chem. Phys.*, 13, 10989–11003, doi:10.5194/acp-13-10989-2013, 2013.
- Aunaas, T.: Nucleating agents in the haemolymph of an intertidal mollusc tolerant to freezing, *Cell. Mol. Life Sci.*, 38, 1456–1457, 1982.
- Berge, O., Monteil, C. L., Bartoli, C., Chandeysson, C., Guilbaud, C., Sands, D. C., and Morris, C. E.: A user's guide to a data base of the diversity of *Pseudomonas syringae* and its application to classifying strains in this phylogenetic complex, *PLOS ONE*, 9, e105547, doi:10.1371/journal.pone.0105547, 2014.
- Berkemeier, T., Shiraiwa, M., Pöschl, U., and Koop, T.: Competition between water uptake and ice nucleation by glassy organic aerosol particles, *Atmos. Chem. Phys.*, 14, 12513–12531, doi:10.5194/acp-14-12513-2014, 2014.

- Brush, R. A., Griffith, M., and Mlynarz, A.: Characterization and quantification of intrinsic ice nucleators in winter rye (*Secale cereale*) leaves, *Plant Physiol.*, 104, 725–735, 1994.
- Budke, C. and Koop, T.: BINARY: an optical freezing array for assessing temperature and time dependence of heterogeneous ice nucleation, *Atmos. Meas. Tech.*, 8, 689–703, doi:10.5194/amt-8-689-2015, 2015.
- Burke, M. J. and Lindow, S. E.: Surface properties and size of the ice nucleation site in ice nucleation active bacteria: theoretical considerations, *Cryobiology*, 27, 88–84, 1990.
- Christner, B. C., Cai, R., Morris, C. E., McCarter, K. S., Foreman, C. M., Skidmore, M. L., Montross, S. N., and Sands, D. C.: Geographic, seasonal, and precipitation chemistry influence on the abundance and activity of biological ice nucleators in rain and snow, *P. Natl. Acad. Sci.*, 105, 18854–18859, 2008a.
- Christner, B. C., Morris, C. E., Foreman, C. M., Cai, R. and Sands, D. C.: Ubiquity of biological ice nucleators in snowfall, *Science*, 319, 1214, doi:10.1126/science.1149757, 2008b.
- Coutinho, T. A. and Venter, S. N.: *Pantoea ananatis*: an unconventional plant pathogen, *Mol. Plant. Pathol.*, 10, 325–335, 2009.
- Deatherage, B. L. and Cookson, B. T.: Membrane vesicle release in bacteria, eukaryotes, and archaea: a conserved yet underappreciated aspect of microbial life, *Infect. Immun.*, 80, 1948–1957, 2012.
- Diehl, K., Quick, C., Matthias-Maser, S., Mitra, S. K., and Jaenicke, R.: The ice nucleation ability of pollen Part I: Laboratory studies in deposition and condensation freezing modes, *Atmos. Res.*, 58, 75–87, 2001.
- Diehl, K., Matthias-Maser, S., Jaenicke, R., and Mitra, S. K.: The ice nucleation ability of pollen Part II: Laboratory studies in immersion and contact freezing modes, *Atmos. Res.*, 61, 125–133, 2002.
- Dreischmeier, K., Budke, C., and Koop, T.: Investigation of heterogeneous ice nucleation in pollen suspensions and washing water, EGU2014-8653, *Geophys. Res. Abstracts*, 16, 2014.
- Duman, J. G., Morris, J. P., and Castellino, F. J.: Purification and composition of an ice nucleating protein from queens of the hornet, *Vespa maculata*, *J. Comp. Physiol. B*, 154, 79–83, 1984.
- Duman, J. G., Neven, L. G., Beals, J. M., Olson, K. R., and Castellino, F. J.: Freeze-tolerance adaptations, including haemolymph protein and lipoprotein nucleators, in the larvae of the crane fly *Tipula trivittata*, *J. Insect Physiol.*, 31, 1–8, 1985.
- Duman, J. G., Wu, D. W., Wolber, P. K., Mueller, G. M., and Neven, L. G.: Further characterization of the lipoprotein ice nucleator from freeze tolerant larvae of the crane fly *Tipula trivittata*, *Comp. Biochem. Physiol.*, 99B, 599–607, 1991.
- Edwards, G. R., Evans, L. F., and La Mer, V. K.: Ice nucleation by monodisperse silver iodide particles, *J. Coll. Sci. Imp. U. Tok.*, 17, 749–758, doi:10.1016/0095-8522(62)90049-1, 1962.
- Erickson, H. P.: Size and shape of protein molecules at the nanometer level determined by sedimentation, gel filtration, and electron microscopy, *Biol. Proced. Online*, 11, 32–51, doi:10.1007/s12575-009-9008-x, 2009.
- Fall, A. L. and Fall, R.: High-level expression of ice nuclei in *Erwinia herbicola* is induced by phosphate starvation and low temperature, *Curr. Microbiol.*, 36, 370–376, 1998.
- Fall, R. and Schnell, R. C.: Association of an ice-nucleating pseudomonad with cultures of the marine dinoflagellate, *Heterocapsa niei*, *J. Marine Res.*, 43, 257–265, 1985.
- Foreman, C. M., Cory, R. M., Morris, C. E., SanClements, M. D., Lisle, J., Miller, P. L., Chin, Y. C., and McKnight, D. M.: Microbial growth under humic-free conditions in a supraglacial stream system on the Cotton Glacier, Antarctica, *Environ. Res. Lett.*, 8, 035022, doi:10.1088/1748-9326/8/3/035022, 2013.
- Fröhlich-Nowoisky, J., Hill, T. C. J., Pummer, B. G., Yordanova, P., Franc, G. D., and Pöschl, U.: Ice nucleation activity in the widespread soil fungus *Mortierella alpina*, *Biogeosciences*, 12, 1057–1071, doi:10.5194/bg-12-1057-2015, 2015.
- Fukuta, N.: Experimental studies of organic ice nuclei, *J. Atmos. Sci.*, 23, 191–196, 1966.
- Gao, W., Smith, D. W., and Sego, D. C.: Ice nucleation in industrial wastewater, *Cold Reg. Sci. Technol.*, 29, 121–133, 1999.
- Garnham, C. P., Campbell, R. L., Walker, V. K., and Davies, P. L.: Novel dimeric β -helical model of an ice nucleation protein with bridged active sites, *BMC Struct. Biol.*, 11, 36, doi:10.1186/1472-6807-11-36, 2011.
- Goldstein, G. and Nobel, P. S.: Changes in osmotic pressure and mucilage during low-temperature acclimation of *Opuntia ficus-indica*, *Plant Physiol.*, 97, 954–961, 1991.
- Goldstein, G. and Nobel, P. S.: Water relations and low-temperature acclimation for cactus species varying in freezing tolerance, *Plant Physiol.*, 104, 675–681, 1994.
- Govindarajan, A. G. and Lindow, S. E.: Size of bacterial ice-nucleation sites measured in situ by radiation inactivation analysis, *P. Natl. Acad. Sci. USA*, 85, 1334–1338, 1988a.
- Govindarajan, A. G. and Lindow, S. E.: Phospholipid requirement for expression of ice nuclei in *Pseudomonas syringae* and in vitro, *J. Biol. Chem.*, 263, 9333–9338, 1988b.
- Graether, S. P. and Jia, Z.: Modeling *Pseudomonas syringae* ice-nucleation proteins as a β -helical protein, *Biophys. J.*, 80, 1169–1173, 2001.
- Graether, S. P., Kulper, M. J., Gagné, S. M., Walker, V. K., Jia, Z., Sykes, B. D., and Davies, P. L.: β -helix structure and ice-binding properties of a hyperactive antifreeze protein from an insect, *Nature*, 406, 325–328, 2000.
- Green, R. L. and Warren, G. J.: Physical and functional repetition in a bacterial ice nucleation gene, *Nature*, 317, 645–648, 1985.
- Griffin, D. W.: Terrestrial microorganisms at an altitude of 20,000 m in Earth's atmosphere, *Aerobiologia*, 20, 135–140, 2004.
- Gross, D. C., Proebsting, E. L., and Maccrindle-Zimmermann, H.: Development, distribution, and characteristics of intrinsic, non-bacterial ice nuclei in *Prunus* wood, *Plant Physiol.*, 88, 915–922, 1988.
- Grote, M., Vrtala, S., Niederberger, V., Wiermann, R., Valenta, R., and Reichelt, R.: Release of allergen-bearing cytoplasm from hydrated pollen: A mechanism common to a variety of grass (Poaceae) species revealed by electron microscopy, *J. Allerg. Clin. Immunol.*, 108, 109–115, doi:10.1067/mai.2001.116431, 2001.
- Grote, M., Valenta, R., and Reichelt, R.: Immunogold scanning electron microscopy of abortive pollen germination: how birch, hazel, and alder release allergenic particles into the atmosphere, *Microsc. Microanal.*, 9, Suppl. S03, 402–403, 2003.
- Gurian-Sherman, D. and Lindow, S. E.: Differential effects of growth temperature on ice nuclei active at different temperatures that are produced by cells of *Pseudomonas syringae*, *Cryobiol.*, 32, 129–138, 1995.

- Haga, D. I., Burrows, S. M., Iannone, R., Wheeler, M. J., Mason, R. H., Chen, J., Polishchuk, E. A., Pöschl, U., and Bertram, A. K.: Ice nucleation by fungal spores from the classes *Agaricomycetes*, *Ustilaginomycetes*, and *Eurotiomycetes*, and the effect on the atmospheric transport of these spores, *Atmos. Chem. Phys.*, 14, 8611–8630, doi:10.5194/acp-14-8611-2014, 2014.
- Hartmann, S., Niedermeier, D., Voigtländer, J., Clauss, T., Shaw, R. A., Wex, H., Kiselev, A., and Stratmann, F.: Homogeneous and heterogeneous ice nucleation at LACIS: operating principle and theoretical studies, *Atmos. Chem. Phys.*, 11, 1753–1767, doi:10.5194/acp-11-1753-2011, 2011.
- Hasegawa, Y., Ishihara, Y., and Tokuyama, T.: Characteristics of ice-nucleation activity in *Fusarium avenaceum* IFO 7158, *Biosci. Biotech. Biochem.*, 58, 2273–2274, 1994.
- Hawksworth, D. L.: The magnitude of fungal diversity: the 1–5 million species estimate revisited, *Mycol. Res.*, 105, 1422–1432, doi:10.1017/S0953756201004725, 2001.
- Hayes, D. R. and Loomis, S. H.: Evidence for a proteinaceous ice nucleator in the hemolymph of the pulmonate gastropod, *Melampus bidentatus*, *Cryo-Lett.*, 6, 418–421, 1985.
- Hiranuma, N., Möhler, O., Yamashita, K., Tajiri, T., Saito, A., Kiselev, A., Hoffmann, N., Hoose, C., Jantsch, E., Koop, T., and Muramaki, M.: Ice nucleation by cellulose and its potential contribution to ice formation in clouds, *Nat. Geosci.*, 8, 273–277, doi:10.1038/ngeo2374, 2015.
- Hoose, C., Kristjánsson, J. E., and Burrows, S. M.: How important is biological ice nucleation in clouds on a global scale? *Environ. Res. Lett.*, 5, 024009, doi:10.1088/1748-9326/5/2/024009, 2010.
- Huffman, J. A., Prenni, A. J., DeMott, P. J., Pöhlker, C., Mason, R. H., Robinson, N. H., Fröhlich-Nowoisky, J., Tobo, Y., Després, V. R., Garcia, E., Gochis, D. J., Harris, E., Müller-Germann, I., Ruzene, C., Schmer, B., Sinha, B., Day, D. A., Andreae, M. O., Jimenez, J. L., Gallagher, M., Kreidenweis, S. M., Bertram, A. K., and Pöschl, U.: High concentrations of biological aerosol particles and ice nuclei during and after rain, *Atmos. Chem. Phys.*, 13, 6151–6164, doi:10.5194/acp-13-6151-2013, 2013.
- Humphreys, T. L., Castrillo, L. A., and Lee, M. R.: Sensitivity of partially purified ice nucleation activity of *Fusarium acuminatum* SRSF 616, *Curr. Microbiol.*, 42, 330–338, doi:10.1007/s002840010225, 2001.
- Iannone, R., Chernoff, D. I., Pringle, A., Martin, S. T., and Bertram, A. K.: The ice nucleation ability of one of the most abundant types of fungal spores found in the atmosphere, *Atmos. Chem. Phys.*, 11, 1191–1201, doi:10.5194/acp-11-1191-2011, 2011.
- Imshenetsky, A. A., Lysenko, S. V., and Kazakov, G. A.: Upper boundary of the biosphere, *Appl. Environ. Microbiol.*, 35, 1–5, 1978.
- Jayaweera, K. and Flanagan, P.: Investigations on biogenic ice nuclei in the Arctic atmosphere, *Geophys. Res. Lett.*, 9, 94–97, 1982.
- Joly, M., Attard, E., Sancelme, M., Deguillaume, L., Guilbaud, C., Morris, C. E., Amato, P., and Delort, A. M.: Ice nucleation activity of bacteria isolated from cloud water, *Atmos. Environ.*, 70, 392–400, 2013.
- Kajava, A. V. and Lindow, S. E.: A model of the three-dimensional structure of ice nucleation proteins, *J. Mol. Biol.*, 232, 709–717, doi:10.1006/jmbi.1993.1424, 1993.
- Katz, U.: Wolkenkammeruntersuchungen der Eiskeimbildungsaktivität einiger ausgewählter Stoffe, *Zeitschr. Angew. Math. Phys.*, 13, 333–358, (in German), 1962.
- Kawahara, H.: The structures and functions of ice crystal-controlling proteins from bacteria, *J. Biosci. Bioengineer.*, 94, 492–496, 2002.
- Kawahara, H., Mano, Y., and Obata, H.: Purification and characterization of extracellular ice-nucleating matter from *Erwinia uredovora* KUIN-3, *Biosci. Biotech. Biochem.*, 57, 1429–1432, 1993.
- Kieft, T. L.: Ice nucleation activity in lichens, *Appl. Environ. Microbiol.*, 54, 1678–1681, 1988.
- Kieft, T. L. and Ahmadjian, V.: Biological ice nucleation activity in lichen mycobionts and photobionts, *Lichenol.*, 21, 355–362, 1989.
- Kieft, T. L. and Ruscetti, T.: Characterization of biological ice nuclei from a lichen, *J. Bacteriol.*, 172, 3519–3523, 1990.
- Kim, H. K., Orser, C., Lindow, S. E., and Sands, D. C.: *Xanthomonas campestris* pv. *translucens* strains active in ice nucleation, *Plant Disease*, 71, 994–997, 1987.
- Koop, T.: Homogeneous Ice Nucleation in Water and Aqueous Solutions, *Zeitschrift für Phys. Chemie*, 218, 1231–1258, doi:10.1524/zpch.218.11.1231.50812, 2004.
- Koop, T. and Zobrist, B.: Parameterizations for ice nucleation in biological and atmospheric systems, *Phys. Chem. Chem. Phys.*, 11, 10741–11064, doi:10.1039/b914289d, 2009.
- Kozloff, L. M., Lute, M., and Westaway, D.: Phosphatidylinositol as a component of the ice nucleating site of *Pseudomonas syringae* and *Erwinia herbicola*, *Science*, 226, 845–846, doi:10.1126/science.226.4676.845, 1984.
- Kozloff, L. M., Turner, M. A., Arellano, F., and Lute, M.: Formation of bacterial membrane ice-nucleating lipoglycoprotein complexes, *J. Bacteriol.*, 173, 2053–2060, 1991.
- Krog, J. O., Zachariassen, K. E., Larsen, B., and Smidsrod, O.: Thermal buffering in Afro-alpine plants due to nucleating agent-induced water freezing, *Nature*, 282, 300–301, doi:10.1038/282300a0, 1979.
- Lagzian, M., Latifi, A. M., Bassami, M. R., Mirzaei, M.: An ice nucleation protein from *Fusarium acuminatum*: cloning, expression, biochemical characterization and computational modeling, *Biotechnol. Lett.*, 36, 2043–2051, doi:10.1007/s10529-014-1568-4, 2014.
- Lindow, S. E., Amy, D. C., and Upper, C. D.: Bacterial ice nucleation - a factor in frost injury to plants, *Plant Physiol.*, 70, 1084–1089, 1982.
- Liou, Y. C., Tocilj, A., Davies, P. L., and Jia, Z.: Mimicry of ice structure by surface hydroxyls and water of a β -helix antifreeze protein, *Nature*, 406, 322–325, 2000.
- Lundheim, R.: Ice nucleation in the blue mussel (*Mytilus edulis*), *Marine Biol.*, 128, 267–271, 1997.
- Macedo, E. A.: Solubility of amino acids, sugars, and proteins, *Pure Appl. Chem.*, 77, 559–568, doi:10.1351/pac200577030559, 2005.
- Madison, D. L., Scrofano, M. M., Ireland, D. C., and Loomis, S. H.: Purification and partial characterization of an ice nucleator protein from the intertidal gastropod, *Melampus bidentatus*, *Cryobiol.*, 28, 483–490, 1991.
- Marcotelli, C., Gedamke, S., Peter, T., and Zobrist, B.: Efficiency of immersion mode ice nucleation on surrogates of mineral dust,

- Atmos. Chem. Phys., 7, 5081–5091, doi:10.5194/acp-7-5081-2007, 2007.
- Möhler, O., Benz, S., Saathoff, H., Schnaiter, M., Wagner, R., Schneider, J., Walter, S., Ebert, V., and Wagner, S.: The effect of organic coating on the heterogeneous ice nucleation efficiency of mineral dust aerosols, *Environ. Res. Lett.*, 3, 025007, doi:10.1088/1748-9326/3/2/025007, 2008.
- Morris, C. E., Sands, D. C., Glaux, C., Samsatly, J., Asaad, S., Moukamel, A. R., Gonçalves, F. L. T., and Bigg, E. K.: Urediospores of rust fungi are ice nucleation active at $> -10^{\circ}\text{C}$ and harbor ice nucleation active bacteria, *Atmos. Chem. Phys.*, 13, 4223–4233, doi:10.5194/acp-13-4223-2013, 2013.
- Mugnano, J. A., Lee, R. E., and Taylor, R. T.: Fat body cells and calcium phosphate spherules induce ice nucleation in the freeze-tolerant larvae of the gall fly *Eurosta solidaginis* (Diptera, Tephritidae), *J. Exp. Biol.*, 199, 465–471, 1996.
- Murase, N., Ruike, M., Matsunaga, N., Hayakawa, M., Kaneko, Y., and Ono, Y.: Spider silk has an ice nucleation activity, *Naturwissenschaften*, 88, 117–118, 2001.
- Murray, B. J., Wilson, T. W., Dobbie, S., Cui, Z., Al-Jumur, S. M. R. K., Möhler, O., Schnaiter, M., Wagner, R., Benz, S., Niemand, M., Saathoff, H., Ebert, V., Wagner, S., and Kärcher, B.: Heterogeneous nucleation of ice particles on glassy aerosols under cirrus conditions, *Nat. Geosci.*, 3, 233–237, doi:10.1038/ngeo817, 2010.
- Nemecek-Marshall, M., LaDuca, R., and Fall, R.: High-level expression of ice nuclei in a *Pseudomonas syringae* strain is induced by nutrient limitation and low temperature, *J. Bacteriol.*, 175, 4062–4070, 1993.
- Neven, L. G., Duman, J. G., Low, M. G., Sehl, L. C., and Castellino, F. J.: Purification and characterization of an insect hemolymph lipoprotein ice nucleator: evidence for the importance of phosphatidylinositol and apolipoprotein in the ice nucleator activity, *J. Comp. Physiol. B*, 159, 71–82, 1989.
- Niedermeier, D., Shaw, R. A., Hartmann, S., Wex, H., Clauss, T., Voigtländer, J., and Stratmann, F.: Heterogeneous ice nucleation: exploring the transition from stochastic to singular freezing behavior, *Atmos. Chem. Phys.*, 11, 8767–8775, doi:10.5194/acp-11-8767-2011, 2011.
- Niedermeier, D., Ervens, B., Clauss, T., Voigtländer, J., Wex, H., Hartmann, S., and Stratmann, F.: A computationally efficient description of heterogeneous freezing: A simplified version of the Soccer ball model, *Geophys. Res. Lett.*, 41, 736–741, 2014.
- Obata, H., Saeki, Y., Tanishita, J., Tokuyama, T., Hori, H., and Higashi, Y.: Identification of an ice-nucleating bacterium KUIN-1 as *Pseudomonas fluorescens* and its ice nucleation properties, *Agric. Biol. Chem.*, 51, 1761–1766, 1987.
- Obata, H., Takinami, K., Tanishita, J., Hasegawa, Y., Kawate, S., Tokutama, T., and Ueno, T.: Identification of a new ice-nucleating bacterium and its ice nucleation properties, *Agric. Biol. Chem.* 53, 725–730, 1990a.
- Obata, H., Takeuchi, S., and Tokuyama, T.: Release of cell-free ice nuclei from *Pseudomonas viridiflava* with a Triton X-100/EDTA system and their ice nucleation properties, *J. Ferment. Bioengineer.*, 70, 308–312, 1990b.
- Obata, H., Tanaka, T., Kawahara, H., and Tokuyama, T.: Properties of cell-free ice nuclei from ice nucleation-active *Pseudomonas fluorescens* KUIN-1, *J. Ferment. Bioengineer.*, 76, 19–24, 1993.
- Ogawa, S., Koga, M., and Osanai, S.: Anomalous ice nucleation behavior in aqueous polyvinyl alcohol solutions, *Chem. Phys. Lett.*, 480, 86–89, 2009.
- Olsen, T. M. and Duman, J. G.: Maintenance of the supercooled state in overwintering pyrochroid beetle larvae, *Dendroides canadensis*: role of hemolymph ice nucleators and antifreeze proteins, *J. Comp. Physiol. B*, 167, 105–113, 1997.
- Osborne, T. B.: Die Pflanzenproteine, *Ergebnisse der Physiologie*, 10, 47–215, (in German), 1910.
- O’Sullivan, D., Murray, B. J., Ross, J. F., Whale, T. F., Price, H. C., Atkinson, J. D., Umo, N. S., and Webb, M. E.: The relevance of nanoscale biological fragments for ice nucleation in clouds, *Scientific Reports*, 5, 8082, doi:10.1038/srep08082, 2015.
- PHELPS, P., GIDDINGS, T. H., PROCHODA, M., and FALL, R.: Release of cell-free ice nuclei by *Erwinia herbicola*, *J. Bacteriol.*, 167, 496–502, 1986.
- Pooley, L. and Brown, T. A.: Preparation of active cell-free ice nuclei from *Pseudomonas syringae*, *P. Roy. Soc. Lond. B*, 24, 112–115, 1990.
- Popovitz-Biro, R., Wang, J. L., Majewski, J., Shavit, E., Leiserowitz, L., and Lahav, M.: Induced freezing of supercooled water into ice by self-assembled crystalline monolayers of amphiphilic alcohols at the air-water interface, *J. Am. Chem. Soc.*, 116, 1179–1191, 1994.
- Pouleur, S., Richard, C., Martin, J. G., and Antoun, H.: Ice nucleation activity in *Fusarium acuminatum* and *Fusarium avenaceum*, *Appl. Environ. Microbiol.*, 58, 2960–2964, 1992.
- Prenni, A. J., Petters, M. D., Faulhaber, A., Carrico, C. M., Ziemann, P. J., Kreidenweis, S. M., and DeMott, P. J.: Heterogeneous ice nucleation measurements of secondary organic aerosol generated from ozonolysis of alkenes, *Geophys. Res. Lett.*, 36, L06808, doi:10.1029/2008GL036957, 2009.
- Pummer, B. G., Bauer, H., Bernardi, J., Bleicher, S., and Grothe, H.: Suspendable macromolecules are responsible for ice nucleation activity of birch and conifer pollen, *Atmos. Chem. Phys.*, 12, 2541–2550, doi:10.5194/acp-12-2541-2012, 2012.
- Pummer, B. G., Atanasova, L., Bauer, H., Bernardi, J., Druzhinina, I. S., Fröhlich-Nowoisky, J., and Grothe, H.: Spores of many common airborne fungi reveal no ice nucleation activity in oil immersion freezing experiments, *Biogeosciences*, 10, 8083–8091, doi:10.5194/bg-10-8083-2013, 2013a.
- Pummer, B. G., Bauer, H., Bernardi, J., Chazallon, B., Facq, S., Lendl, B., Whitmore, K., and Grothe, H.: Chemistry and morphology of dried-up pollen suspension residues, *J. Raman Spectrosc.*, 44, 1654–1658, doi:10.1002/jrs.4395, 2013b.
- Richard, C., Martin, J. G., and Pouleur, S.: Ice nucleation activity identified in some phytopathogenic *Fusarium* species, *Phytoprotection*, 77, 83–92, 1996.
- Rogers, J. S., Stall, R. E., and Burke, M. J.: Low-temperature conditioning of the ice nucleation active bacterium, *Erwinia herbicola*, *Cryobiol.*, 24, 270–279, 1987.
- Santl-Temkiv, T., Sahyoun, M., Finster, K., Hartmann, S., Augustin, S., Stratmann, F., Wex, H., Clauss, T., Nilsen, N. W., Sørensen, J. H., Korsholm, U. S., Wick, L. Y., and Karlson, U. G.: Characterization of airborne ice-nucleation-active bacteria and bacterial fragments, *Atmos. Environ.*, 109, 105–117, doi:10.1016/j.atmosenv.2015.02.060, 2015.

- Sattler, B., Puxbaum, H., and Psenner, R.: Bacterial growth in supercooled cloud droplets, *Geophys. Res. Lett.*, 28, 239–242, doi:10.1029/2000GL011684, 2001.
- Schäppi, G. F., Suphioglu, C., Taylor, P. E., and Knox, R. B.: Concentrations of the major birch tree allergen Betv1 in pollen and respirable fine particles in the atmosphere, *J. Allerg. Clin. Immunol.*, 100, 656–661, 1997.
- Schill, G. P., De Haan, D. O., and Tolbert, M. A.: Heterogeneous ice nucleation on simulated secondary organic aerosol, *Environ. Sci. Technol.*, 48, 1675–1682, doi:10.1021/es4046428, 2014.
- Schmid, D., Pridmore, D., Capitani, G., Battistutta, R., Neeser, J. R., and Jann, A.: Molecular organization of the ice nucleation protein InaV from *Pseudomonas syringae*, *FEBS Lett.*, 414, 590–594, 1997.
- Solomon, W. R., Burge, H. A., and Muilenberg, M. L.: Allergen carriage by atmospheric aerosol. I. Ragweed pollen determinants in smaller micronic fractions, *J. Allerg. Clin. Immunol.*, 72, 443–447, 1983.
- Stakman, E. and Christensen, C. M.: Aerobiology in relation to plant disease, *Botan. Rev.*, 12, 205–253, 1946.
- Tsumuki, H. and Konno, H.: Ice nuclei produced by *Fusarium* sp. isolated from the gut of the rice stem borer, *Chilo suppressalis* Walker (Lepidoptera: Pyralidae), *Biosci. Biotech. Biochem.*, 58, 578–579, 1994.
- Tsumuki, H., Yanai, H., and Aoki, T.: Identification of ice-nucleating active fungus isolated from the gut of the rice stem borer, *Chilo suppressalis* Walker (Lepidoptera: Pyralidae) and a search for ice-nucleating active *Fusarium* species, *Ann. Phytopathol. Soc. Jpn.*, 61, 334–339, 1995.
- Turner, M. A., Arellano, F., and Kozloff, L. M.: Components of ice nucleation structures of bacteria, *J. Bacteriol.*, 173, 6515–6527, 1991.
- Vaitilingom, M., Attard, E., Gaiani, N., Sancelme, M., Deguillaume, L., Flossmann, A. I., Amato, P., and Delort, A.-M.: Long-term features of cloud microbiology at the puy de Dôme (France), *Atmos. Environ.*, 56, 88–100, 2012.
- Vali, G.: Quantitative evaluation of experimental results on the heterogeneous freezing nucleation of supercooled liquids, *J. Atmos. Sci.*, 28, 402–409, 1971.
- van Eaton, A. R., Harper, M. A., and Wilson, C. J. N.: High-flying diatoms: Widespread dispersal of microorganisms in an explosive volcanic eruption, *Geology*, 41, 1187–1190, doi:10.1130/G34829.1, 2013.
- von Blohn, N., Mitra, S. K., Diehl, K., and Borrmann, S.: The ice nucleating ability of pollen. Part III: New laboratory studies in immersion and contact freezing modes including more pollen types, *Atmos. Res.*, 78, 182–189, 2005.
- Wagner, R., Möhler, O., Saathoff, H., Schnaiter, M., and Leisner, T.: New cloud chamber experiments on the heterogeneous ice nucleation ability of oxalic acid in the immersion mode, *Atmos. Chem. Phys.*, 11, 2083–2110, doi:10.5194/acp-11-2083-2011, 2011.
- Wang, B. and Knopf, D. A.: Heterogeneous ice nucleation on particles composed of humic-like substances impacted by O₃, *J. Geophys. Res.*, 116, D03205, doi:10.1029/2010JD014964, 2011.
- Wang, B., Lambe, A. T., Massoli, P., Onasch, T. B., Davidovits, P., Worsnop, D. R., and Knopf, D. A.: The deposition ice nucleation and immersion freezing potential of amorphous secondary organic aerosol: Pathways for ice and mixed-phase cloud formation, *J. Geophys. Res.*, 117, D16209, doi:10.1029/2012JD018063, 2012.
- Warren, G. and Wolber, P.: Molecular aspects of microbial ice nucleation, *Mol. Microbiol.*, 5, 239–243, 1991.
- Welti, A., Lüönd, F., Kanji, Z. A., Stetzer, O., and Lohmann, U.: Time dependence of immersion freezing: an experimental study on size selected kaolinite particles, *Atmos. Chem. Phys.*, 12, 9893–9907, doi:10.5194/acp-12-9893-2012, 2012.
- Wilson, T. W., Murray, B. J., Wagner, R., Möhler, O., Saathoff, H., Schnaiter, M., Skrotzki, J., Price, H. C., Malkin, T. L., Dobbie, S., and Al-Jumur, S. M. R. K.: Glassy aerosols with a range of compositions nucleate ice heterogeneously at cirrus temperatures, *Atmos. Chem. Phys.*, 12, 8611–8632, doi:10.5194/acp-12-8611-2012, 2012.
- Wolanczyk, J. P., Storey, K. B., and Baust, J. G.: Ice nucleating activity in the blood of the freeze-tolerant frog, *Rana sylvatica*, *Cryobiol.*, 27, 328–335, 1990.
- Xu, H., Griffith, M., Patten, C. L., and Glick, B. R.: Isolation and characterization of an antifreeze protein with ice nucleation activity from the plant growth promoting rhizobacterium *Pseudomonas putida* GR12-2, *Can. J. Microbiol.*, 44, 64–73, doi:10.1139/w97-126, 1998.
- Yttri, K. E., Dye, C., and Kiss, G.: Ambient aerosol concentrations of sugars and sugar-alcohols at four different sites in Norway, *Atmos. Chem. Phys.*, 7, 4267–4279, doi:10.5194/acp-7-4267-2007, 2007.
- Zachariassen, K. E. and Kristiansen, E.: Ice nucleation and antinucleation in nature, *Cryobiol.*, 41, 257–279, 2000.
- Zobrist, B., Marcolli, C., Koop, T., Luo, B. P., Murphy, D. M., Lohmann, U., Zardini, A. A., Krieger, U. K., Corti, T., Cziczo, D. J., Fueglistaler, S., Hudson, P. K., Thomson, D. S., and Peter, T.: Oxalic acid as a heterogeneous ice nucleus in the upper troposphere and its indirect aerosol effect, *Atmos. Chem. Phys.*, 6, 3115–3129, doi:10.5194/acp-6-3115-2006, 2006.
- Zobrist, B., Koop, T., Luo, B. P., Marcolli, C., and Peter, T.: Heterogeneous ice nucleation rate coefficient of water droplets coated by a nonadecanol monolayer, *J. Phys. Chem. C*, 111, 2149–2155, 2007.
- Zuberi, B., Bertram, A. K., Koop, T., Molina, L. T. and Molina, M. J.: Heterogeneous Freezing of Aqueous Particles Induced by Crystallized (NH₄)₂SO₄, Ice, and Letovicite, *J. Phys. Chem. A*, 105, 6458–6464, doi:10.1021/jp010094e, 2001.

Supplement of Atmos. Chem. Phys., 15, 4077–4091, 2015
<http://www.atmos-chem-phys.net/15/4077/2015/>
doi:10.5194/acp-15-4077-2015-supplement
© Author(s) 2015. CC Attribution 3.0 License.



Supplement of

Ice nucleation by water-soluble macromolecules

B. G. Pummer et al.

Correspondence to: B. G. Pummer (b.pummer@mpic.de)

1 **S1 Theoretical considerations**

2 **S1.1 Macromolecules and solubility**

3 Macromolecules are per definition molecules with a molecular mass of >10 kg/mol (Staudinger
4 and Staudinger, 1954), which is equivalent to >10 kDa. In contrast to crystals or metals, which
5 consist of subunits that are held together by non-covalent forces (e.g. ionic, metal or dipole
6 bonds), each atom of a macromolecule is covalently bound to the rest of the molecule. Since
7 covalent bonds are usually much stronger than non-covalent bonds, they stay intact in solution.
8 In contrast, a sodium chloride crystal is broken down into single sodium cations and chloride
9 anions and thereby loses its former structure. The variety of macromolecules ranges from
10 inorganic (e.g. diamond, silicate) to organic (e.g. plastics) to biological (e.g. proteins,
11 polysaccharides, sporopollenin, lignin) exponents.

12 Polymers are a subgroup of macromolecules, which are built up by a chain of covalently linked
13 small molecules. Such a molecular chain will not stay linear, but will fold into a more compact
14 form – especially if it contains hydrophobic elements in a hydrophilic surrounding or the other
15 way round. This folding can be either random or in a well-defined manner. Proteins in their
16 functional state usually have a very distinct folding. Protein chains that are not properly folded
17 lack in most cases their functionality. Since the non-covalent forces holding the protein structure
18 intact are usually weak, stress treatments lead to unfolding and therefore inactivation of the
19 protein.

20 The solubility of a macromolecule depends on the chemistry of the macromolecule and the
21 solvent. Based on the protein classification approach by T. B. Osborne (Osborne, 1910)
22 biological matter is suspended and shaken in a certain solvent. Then the matter is centrifuged or
23 filtrated off, thus removing particulate matter and yielding a transparent supernatant. Molecules
24 that are extracted into the supernatant are considered to be soluble in that medium.

25 In the case of large molecules, it is disputable where to draw the line between solution and
26 suspension. Per definition, a solution consists of a single phase, while a suspension consists of
27 two phases with phase interfaces. If the particles sizes are close to the wavelength of visible
28 light, a suspension shows light scattering, which makes it opaque. A solution, in contrast, shows
29 neither light scattering, nor visible particles. Furthermore, a solution shows no phase separation

1 over time, while sedimentation or agglutination lead to a progressive phase separation in time.
2 Additionally, solutions cannot be separated by centrifugation. From a molecular point of view, a
3 molecule in solution is fully covered with an energetically favorable hydration shell.

4

5 **S1.2 Basic physics of INA**

6 At temperatures below the melting point (273.15 K at atmospheric pressure), ice is
7 thermodynamically favored over liquid water. Nevertheless, the spontaneous freezing of liquid
8 water that is supercooled below this point is statistically very unlikely, because the phase
9 transition is kinetically hindered. To form ice, water molecules have to be arranged in a defined
10 ice crystal structure instead of the more random orientation and translational degrees of freedom
11 they have in a liquid. Due to energetic propitiousness, which comes from the crystallization
12 energy, clusters of a few water molecules will tend to arrange in an ice-like structure in the liquid
13 water body. These clusters, which are also known as ice embryos, however, are then ripped apart
14 by their surface tension, so in supercooled water, there is equilibrium between formation and
15 decay of ice embryos.

16 Crystallization energy is proportional to the volume of the ice embryo, and therefore to the radius
17 cubed. In contrast surface tension is proportional to the surface, and therefore to the radius
18 squared. The outcome of the battle between crystallization energy and surface tension depends
19 on the value of the Gibbs Energy ΔG , which is therefore a function of the radius r (see Eq.(S1)),
20 in other words the size of the water molecule cluster. $\Delta G(r)$ initially increases with r , then
21 reaches a maximum ΔG^* , which is equivalent to the activation energy of the process (see
22 Eq.(S2)). After that, ΔG strongly decreases with r . Once the critical radius r^* (see Eq.(S3)) is
23 reached, meaning that the activation barrier ΔG^* is overcome, the ice embryo will grow
24 unimpededly and subsequently catalyze the freezing of the entire supercooled body of water.

25 The critical ice embryo size in turn depends on the temperature, decreasing in size as the
26 intensity of supercooling increases, or, in other words as the temperatures drop below 273.15 K.
27 For example, 45000 arranged water molecules constitute the critical ice embryo size at 268 K,
28 while only 70 are required at 233 K (Zachariassen and Kristiansen, 2000). Furthermore, the
29 probability of forming a cluster decreases with its size. Therefore, freezing becomes very
30 unlikely at higher temperatures (so far we take only water molecules into account). This situation

1 is the basis of why ultrapure water can be cooled down to temperatures about 235 K before it
2 will eventually freeze. The manifestation of a critical ice embryo, which eventually leads to ice
3 formation, is called ice nucleation. When only water molecules are involved, it is called
4 homogeneous ice nucleation (see Fig. 1a).

$$5 \quad \Delta G = 4\pi \cdot \gamma \cdot r^2 + \frac{4}{3}\pi \cdot \rho \cdot \Delta\mu \cdot r^3 \quad (S1)$$

$$6 \quad \Delta G^* = \frac{16\pi \cdot \gamma^3}{3 \cdot \rho^2 \cdot (\Delta\mu)^2} \quad (S2)$$

$$7 \quad r^* = -\frac{2 \cdot \gamma}{\rho \cdot \Delta\mu} \quad (S3)$$

8 ΔG ...Gibbs energy, r ...cluster radius, γ ... surface free energy, ρ ...bulk density, $\Delta\mu$...phase
9 transition chemical potential, ΔG^* ...activation energy, r^* ...critical radius

10 The probability of freezing increases when water contains or comes in contact with structured
11 surfaces that simulate ice and arrange water molecules in an ice-like manner. This stabilizes ice
12 embryos, and therefore decreases the activation barrier in the manner of a catalyst. These ice-
13 template structures are known as ice nucleators (INs) or ice nuclei, and the process they catalyze
14 is known as heterogeneous ice nucleation (see Fig. 1b+c). The driving force of the arrangement
15 of water molecules on IN surfaces is interaction between the partially charged ends of the water
16 molecule and oppositely charged functional groups on the IN surface. This involves H-bonds
17 between hydrogen atoms with partial positive charges and oxygen or nitrogen atoms with partial
18 negative charges. Therefore, the IN has to carry functional groups at the proper position to be
19 effective (Liou et al., 2000, Zachariassen and Kristiansen, 2000). In most cases only certain
20 sections, which are known as “active sites”, participate in the INA, while the majority of the IN
21 surface is inactive (Edwards et al., 1962, Katz, 1962).

22 The larger the active site of an IN, and the more fitting functional groups it carries, the more
23 effective it stabilizes clusters, and so the higher the freezing temperature. Consequently, single
24 molecules of low-molecular compounds cannot nucleate ice. In fact, soluble compounds
25 consisting of very small molecules or ions, like salts, sugars or short-chained alcohols, cause a
26 freezing point depression. However, if single molecules are very large, they can allocate enough
27 active surface to be INs by themselves. Such ice nucleating macromolecules (INMs) are
28 especially common among biological INs. Due to the same reason some low-molecular organic

1 compounds which do not induce ice formation in solution, can act as IN, if they are crystallized
2 in layers of a certain arrangement (Fukuta, 1966).

3

4 **S1.3 INA modes**

5 Throughout the manuscript we present the physics of ice nucleation mainly with regard to
6 immersion freezing where the IN is inside a cooling water droplet. But in fact, three more modes
7 of ice nucleation are defined. Immersion freezing is the most-investigated mode, and is suspected
8 to be the dominant ice formation mechanism in mixed-phase clouds (Ansmann et al., 2009,
9 Wiacek et al., 2010, de Boer et al., 2011). The other modes are contact, deposition and
10 condensation ice nucleation. Contact ice nucleation means that the IN collides with a
11 supercooled droplet, which freezes on contact. Deposition ice nucleation is adsorption of water
12 vapor on the IN surface as ice, and condensation ice nucleation is condensation of water vapor as
13 liquid layer on the IN, which then freezes at the same temperature. Deposition ice nucleation is
14 somewhat different, since the water molecules from the gas phase have to be arranged, while in
15 the other modes freezing occurs in the liquid phase. Consequently, some particles that have
16 shown ice nucleation activity (INA) in the other three modes are inactive in the deposition mode
17 (Diehl et al., 2001, Diehl et al., 2002). Condensation and deposition mode depend additionally on
18 atmospheric pressure and humidity, which play no role, if ice nucleation occurs in pre-existing
19 droplets. For condensation mode activity, the IN additionally has to carry hygroscopic functional
20 groups, which also make it an efficient cloud condensation nucleus (CCN). Since all four modes
21 are theoretical models, they are permanently under discussion. Debates go so far as to question
22 not only the real-life relevance, but also the existence itself of some modes. For example, one
23 could claim that a condensation IN is consecutively acting as a CCN and an immersion IN
24 (Fukuta and Schaller, 1982, Wex et al., 2014). In light of this debate we focus only on immersion
25 freezing.

26

27 **S1.4 Water activity**

28 It is possible to view INA in the light of the water activity (a_w). The thermodynamic freezing and
29 melting temperature of water (T_m), which is independent of insoluble INs, is a function of a_w . A

1 reduction of a_w due to the addition of solutes leads to a freezing point depression, as it is
2 illustrated in Fig. S1. The effective freezing / ice nucleation temperature shows the same
3 dependence on a_w , but is horizontally shifted relative to the $T_m(a_w)$ -curve (Zobrist et al., 2008,
4 Koop and Zobrist, 2009). The distance between the ice nucleation and melting curve at a given
5 temperature is named Δa_w , which is the measure of the INA of a water sample. For example, for
6 the homogeneous freezing on IN-free samples, Δa_w is about 0.31 ± 0.02 (Koop et al., 2000, Koop
7 and Zobrist, 2009). The addition of IN in the water leads to a horizontal shift of the ice
8 nucleation curve towards the melting curve, or a reduction in Δa_w . In the experiment, a
9 nucleation spectrum of a water droplet ensemble with given INA and a given a_w is like a vertical
10 trajectory going through the phase diagram in Fig. S1 from top to bottom. Therefore, the ice
11 nucleation temperature depends on both the present INs and a_w .

12 Instead of assigning a certain ice nucleation temperature to a sample, it is more accurate for
13 stochastic, time-dependent INs to assign nucleation rate coefficients $J(T, a_w)$, which increase with
14 decreasing T and increasing a_w (Knopf and Alpert, 2013). Therefore, one can add J contour lines
15 to Fig. S1, which show the same shape as the thermodynamic and the homogeneous freezing
16 curve (Koop et al., 2000, Attard et al., 2012, Knopf and Alpert, 2013). This means that from the
17 thermodynamic freezing line to the homogeneous freezing line we have a gradient of increasing
18 J . Accordingly, cooling is a steady increase in J . This makes J independent of the absolute
19 freezing temperature, and therefore of the IN type.

20

21 **S1.5 Motivation for expression of biological INMs**

22 There are several theories addressing the question of why some organisms produce IN. Overall,
23 it is proposed that INA is a form of adaption for survival or enhanced fitness in cold
24 environments. More than 80% of the total biosphere volume is exposed to temperatures below
25 278 K, thriving either in the oceans or in frosty regions (Christner 2010). Also in temperate
26 climate zones, temperatures can regularly drop below the freezing point. The formation of ice
27 crystals can pierce cell walls and membranes, which leads to loss of cell fluids. Consequently,
28 adaptations for either avoiding or managing freezing make sense for the many species that are
29 exposed to such hostile conditions. The correlation between the INA of bacteria and the
30 geographic latitude that was found by Schnell and Vali (1976) supports the idea of a selective

1 advantage for organisms with INA in cold environments. For the γ -Proteobacteria the gene for
2 the BINM most likely originates from the common ancestor of this class of bacteria and
3 therefore has been part of the genome of these organisms for at least 0.5 to 1.75 billion years
4 (Morris et al., 2014). To be maintained for this length of time, the gene is likely to be under
5 positive natural selection because it confers a fitness advantage. The possible advantages that
6 have been proposed are:

- 7 (i) Nutrient mining (Lindow et al., 1982): Highly active INMs were mainly found in
8 plant pathogenic species (bacteria, *Fusarium*, rust fungi) or in lichen. By inciting the
9 growth of ice crystals, these organisms can essentially “dig” into the substrate on
10 which they are growing (mainly plant tissues, but also rocks in the case of lichens),
11 thereby acquiring nutrients.
- 12 (ii) Cryoprotection (Krog et al., 1979, Duman et al., 1992): The INA of plants and
13 animals, but possibly also of lichens, is protective against frost injury. Ice growth in
14 organisms is dangerous, because it ruptures the sensitive cell membranes thereby
15 damaging or killing the cells. If the ice is formed on a less sensitive location, such as
16 outside of the cells (e.g. in intercellular fluids), the danger of frost injury is far lower.
17 Forming ice on the INMs prevents further ice formation at other places – partly
18 because of the change in water activity, but also due to the release of crystallization
19 heat, which prevents a further temperature decrease. This might explain why most
20 known biological INMs are extracellular (see Table 1), and why they are active at
21 such high temperatures, where the heat of fusion is sufficient to warm the cells to
22 survivable temperatures.
- 23 (iii) Water reservoir (Kieft and Ahmadjian, 1989): Ice crystals might serve as water
24 storage in cold and dry environments. The form stability of ice and its low vapor
25 pressure reduce the potential loss of water in comparison to the loss from liquid water
26 droplets.
- 27 (iv) Cloud seeding to assure deposition (Morris et al., 2008, 2013a, 2013b): The lifecycles
28 of some species involve long distance dissemination that takes them up into clouds
29 but where they will not proliferate unless they return to Earth’s surface. Particles that
30 attain cloud height are generally too small to deposit due to their own weight.

1 Therefore, they require means of active deposition, such as precipitation that forms
2 from ice initiated in clouds via ice nucleation.

3 (v) Incidental (Lundheim 2002): In some cases, INA was detected where it cannot be
4 explained by any reason. In this case, the INA might be an accidental property of a
5 bioparticle that has another function in the organism. For example, the low density
6 lipoproteins in human blood show INA, although their purpose lies in fat metabolism.

7 Advantages (i) and (ii) might be distinguishable by the freezing temperature (Duman et al.,
8 1992): Since (i) demands ice formation as soon as possible, and the formation of few large ice
9 crystals, such INMs are active at a very high temperature. On the other hand, type-(ii)-INMs are
10 active at lower temperatures, only before other parts of the organism would start freezing.
11 Furthermore, less efficient IN favor formation of smaller, less sharp and damaging ice crystals
12 than those formed by type-(i)-INMs.

13

14 **S1.6 Mineral dust IN**

15 Apart from biological INMs, some types of mineral dust and soot have shown INA in different
16 laboratory experiments (e.g. Murray et al., 2012), what might make them relevant for
17 atmospheric ice formation.

18 Among mineral dust, potassium feldspar and fluorine phlogopite (a type of potassium micas)
19 showed by far the highest INA (Shen et al., 1977, Atkinson et al., 2013, Augustin-Bauditz et al.,
20 2014, Zolles et al., 2015). The reason for this higher accentuated activity compared to other
21 closely related minerals is thought to be due to the potassium cations, whose hydration shell
22 density matches that of ice. In contrast, the hydration shells of sodium and calcium ions are far
23 tighter due to the higher ion charge density. So they likely disturb the ice-like water molecule
24 arrangement, while potassium is neutral or supportive (Shen et al., 1977). It should be pointed
25 out that this hypothesis is not valid for low molecular weight compounds. Soluble potassium
26 salts (e.g. KCl, KNO₃, etc.) lead to a freezing point depression, as do salts with other cations. In
27 the crystal lattice of feldspar the ions are fixed in a confined geometry that seems to match the
28 ice crystal lattice. This probably causes the INA. Other ions with the same charge and the
29 approximately same diameter, for example ammonium, might also have a favorable effect on the
30 INA. It is interesting to note that several studies suggest that traces of ammonium contaminants

1 in silver iodine increase its INA (e.g. Corrin et al., 1964, Steele and Krebs, 1966, Bassett et al.,
2 1970).

3

4 **S2 Details about methods**

5 **S2.1 Molecular modeling**

6 The insect antifreeze protein (AFP) from the beetle *Tenebrio molitor* was simulated (see Fig. 1c).
7 The 8.4 kDa AFP is composed of 12-residue repeats and is stabilized by disulfide- bonds in the
8 core of the protein. A defined structure of six parallel beta-sheets built up from the sequence
9 TCT shows a high ordered surface to the water. The starting structure was taken from the *Protein*
10 *Data Bank* (Liou et al., 2000), protonated with “prontonate3d” from the MOE2013.08 modeling
11 package, and solvated in TIP4P-2005 water (Abascal and Vega, 2005) with 12 Å wall separation.
12 Minimization and equilibration were performed according to Wallnoefer et al. (2010). Then 100
13 nanoseconds of NpT (isothermal and isobaric) molecular dynamics simulation at 220 K were
14 recorded using an 8 Å cutoff for non-bonded interaction and the *Particle Mesh Ewald* algorithm
15 for treating long-range electrostatics (Darden et al., 1993).

16 Water Analysis: Snapshots were taken every picosecond, and water density was estimated as
17 described by Huber et al.(2013). Afterwards, the most likely water positions were extracted.
18 During the simulation of 1EZG a very well structured first layer of water, which we colored blue,
19 could be observed. Water less structured than the first layer was colored red.

20

21 **S2.2 Size exclusion chromatography**

22 High-purity water (18.2 MΩ·cm) was taken from an ELGA LabWater system (PURELAB Ultra,
23 ELGA LabWater Global Operations, UK). Ammonium acetate (NH₄Ac; ≥ 98%, puriss p.a.), DL-
24 dithiothreitol (DTT; > 99%), iodoacetamide (IAM; ≥ 99%), 2,2,2-trifluoroethanol (TFE; ≥ 99%,
25 ReagentPlus), ammonium bicarbonate (NH₄HCO₃; ≥ 99%, ReagentPlus), Trypsin from porcine
26 pancreas (proteomics grade) and protein standard mix (15–600 kDa) were obtained from Sigma
27 Aldrich, Steinbach, Germany. Formic acid (FA; > 99%, for analysis) was from Acros Organics,
28 Geel, Belgium. Guanidinium chloride was from Promega, Madison, WI, USA.

1 The HPLC-DAD system consisted of a binary pump (G1379B), an autosampler with thermostat
2 (G1330B), a column thermostat (G1316B), and a photo-diode array detector (DAD; G1315C)
3 from Agilent Technologies (Waldbronn, Germany). Chemstation software (Rev. B.03.01,
4 Agilent) was used for system control and data analysis. A size exclusion column (Agilent Bio
5 SEC-3, 300 Å, 4.6 x 150 mm, 3 µm particle size) with exclusion limits of 5 kDa to 1.25 MDa
6 was used for chromatographic separation. 50 mM NH₄Ac in ultrapure water (pH 6.7) was used
7 as the eluent. Isocratic analyses with a runtime of 10 min were performed at 303 K with a flow
8 rate of 350 µL min⁻¹. After each measurement the column was flushed for 5 min with the same
9 eluent before the next run. Absorbance was monitored at wavelengths of 220 and 280 nm. The
10 sample injection volume was 40 µL. Sample fractions were collected at different retention time
11 intervals corresponding to different molecular weight intervals as shown in Table S1. Molecular
12 weights are calculated according to a protein standard mix with four calibration points ranging
13 from 15 to 600 kDa. To get rid of the residues from the birch pollen extract, the column was
14 cleaned after each work day with 6 M guanidinium chloride overnight, and then with pure water.

15 The protocol for the protein digestion was as follows: 5 µL of a 100 mM NH₄HCO₃ solution and
16 5 µL TFE were added to 100 µL of sample. Then 0.5 µL 200 mM DTT solution were added, the
17 sample was briefly vortexed and then incubated for 1 h at 333 K to denature the proteins. After
18 letting the sample cool to room temperature 2 µL of 200 mM IAM solution were added and the
19 sample was allowed to stand for 1h in the dark (covered with aluminum foil) to alkylate the
20 protein cysteine residues. The sample was allowed to stand for another hour in the dark after
21 adding 0.5 µL 200 mM DTT solution to destroy excess IAM. Now 60 µL autoclaved water and
22 20 µL 100 mM NH₄HCO₃ solution were added to adjust the sample pH for digestion. Two
23 microliters of 1 µg/µL Trypsin in 50 mM acetic acid was added and the sample was incubated at
24 310 K for 18 h. To stop the digestion 0.5 µL FA were added. The procedure for the treatment of
25 samples and controls is given in Table 2.

26

27 **References (Supplement)**

28 Abascal, J. L. F., and Vega, C.: A general purpose model for the condensed phases of water:
29 TIP4P/2005, J. Chem. Phys., 123, 234505, doi:10.1063/1.2121687, 2005. Ansmann, A., Tesche,
30 M., Seifert, P., Althausen, T., Engelmann, R., Fruntke, J., Wandinger, U., Mattis, I., and Müller,

1 D.: Evolution of the ice phase in tropical altocumulus: SAMUM lidar observations over Cape
2 Verde, *J. Geophys. Res.*, 114, D17208, doi:10.1029/2008JD011659, 2009.

3 Atkinson, J. D., Murray, B. J., Woodhouse, M. T., Whale, T. F., Baustian, K. J., Carlslaw, K. S.,
4 Dobbie, S., O'Sullivan, D., and Malkin, T. L.: The importance of feldspar for ice nucleation by
5 mineral dust in mixed-phase clouds, *Nature*, 498, 355-358, 2013.

6 Attard, E., Yang, H., Delort, A.-M., Amato, P., Pöschl, U., Glaux, C., Koop, T., and Morris, C. E.:
7 Effects of atmospheric conditions on ice nucleation activity of *Pseudomonas*, *Atmos. Chem.*
8 *Phys.*, 12, 10667-10677, doi:10.5194/acp-12-10667-2012, 2012.

9 Augustin-Bauditz, S., Wex, H., Kanter, S., Ebert, M., Stolz, F., Prager, A., Niedermeier, D., and
10 Stratmann, F.: The immersion mode ice nucleation behavior of mineral dusts: A comparison of
11 different pure and surface modified dusts, *Geophys. Res. Lett.*, 41, 7375-7382,
12 doi:10.1002/2014GL061317, 2014.

13 Bassett, D. R., Boucher, E. A., and Zettlemoyer, A. C.: Adsorption studies on ice-nucleating
14 substrates. Hydrophobed silicas and silver iodide, *J. Colloid Interfac. Sci.*, 34, 436-446, 1970.

15 Christner, B. C.: Bioprospecting for microbial products that affect ice crystal formation and
16 growth, *Appl. Microbiol. Biotech.*, 85, 481-489, 2010.

17 Corrin, M. L., Edwards, H. W., and Nelson, J. A.: The surface chemistry of condensation nuclei:
18 II. The preparation of silver iodide free of hygroscopic impurities and its interaction with water
19 vapor, *J. Atmos. Sci.*, 21, 565-567, 1964.

20 Darden, T., York, D., and Pedersen, L.: Particle mesh Ewald: An $N \cdot \log(N)$ method for Ewald
21 sums in large systems, *J. Chem. Phys.*, 98, 10089-10092, doi:10.1063/1.464397, 1993.

22 de Boer, G., Morrison, H., Shupe, M. D., and Hildner, R.: Evidence of liquid dependent ice
23 nucleation in high-latitude stratiform clouds from surface remote sensors, *Geophys. Res. Lett.*,
24 38, L01803, doi:10.1029/2010GL046016, 2011.

25 Diehl, K., Quick, C., Matthias-Maser, S., Mitra, S. K., and Jaenicke, R.: The ice nucleation
26 ability of pollen Part I: Laboratory studies in deposition and condensation freezing modes,
27 *Atmos. Res.*, 58, 75-87, 2001.

28 Diehl, K., Matthias-Maser, S., Jaenicke, R., and Mitra, S.K.: The ice nucleation ability of pollen

1 Part II. Laboratory studies in immersion and contact freezing modes, *Atmos. Res.*, 61, 125-133,
2 2002.

3 Duman, J. G., Wu, D. W., Yeung, K. L., and Wolf, E. E.: Hemolymph proteins involved in the
4 cold tolerance of terrestrial arthropods: antifreeze and ice nucleator proteins, *Water and Life*,
5 Springer Berlin Heidelberg, ISBN-13: 9783540541127, 282-300, 1992.

6 Edwards, G. R., Evans, L. F., and La Mer, V. K.: Ice nucleation by monodisperse silver iodide
7 particles, *J. Colloid Sci.*, 17, 749-758, doi:10.1016/0095-8522(62)90049-1, 1962.

8 Fukuta, N.: Experimental studies of organic ice nuclei, *J. Atmos. Sci.*, 23, 191-196, 1966.

9 Fukuta, N., and Schaller, R.C.: Ice nucleation by aerosol particles: Theory of condensation-
10 freezing nucleation, *J. Atmos. Sci.*, 39, 648-655, 1982.

11 Huber, R. G., Fuchs, J. E., von Grafenstein, S., Laner, M., Wallnoefer, H. G., Abdelkader, N., and
12 Liedl, K. R.: Entropy from state probabilities: hydration entropy of cations, *J. Phys. Chem. B*,
13 117, 6466-6472, doi:10.1021/jp311418q, 2013.

14 Katz, U.: Wolkenkammeruntersuchungen der Eiskeimbildungsaktivität einiger ausgewählter
15 Stoffe, *Zeitschr. Angew. Math. Phys.*, 13, 333-358, 1962. (in German)

16 Kieft, T. L., and Ahmadjian, V: Biological ice nucleation activity in lichen mycobionts and
17 photobionts, *Lichenol.*, 21, 355-362, 1989.

18 Knopf, D. A., and Alpert, P. A.: A water activity based model of heterogeneous ice nucleation
19 kinetics for freezing of water and aqueous solution droplets, *Faraday Discuss.*, 165, 513-534,
20 doi:10.1039/c3fd00035d, 2013.

21 Koop, T., Luo, B., Tsias, A., and Peter, T.: Water activity as the determinant for homogeneous ice
22 nucleation in aqueous solutions, *Nature*, 406, 611-614, 2000.

23 Koop, T., and Zobrist, B.: Parameterizations for ice nucleation in biological and atmospheric
24 systems, *Phys. Chem. Chem. Phys.*, 11, 10741-11064, doi:10.1039/b914289d, 2009.

25 Krog, J. O., Zachariassen, K. E., Larsen, B., and Smidsrod, O.: Thermal buffering in Afro-alpine
26 plants due to nucleating agent-induced water freezing, *Nature*, 282, 300-301,
27 doi:10.1038/282300a0, 1979.

28 Lindow, S.E., Amy, D.C., and Upper, C.D.: Bacterial ice nucleation - a factor in frost injury to

1 plants, *Plant Physiol.*, 70, 1084-1089, 1982.

2 Liou, Y.C., Tocilj, A., Davies, P.L., and Jia, Z.: Mimicry of ice structure by surface hydroxyls and
3 water of a β -helix antifreeze protein, *Nature*, 406, 322-325, 2000.

4 Lundheim, R.: Physiological and ecological significance of biological ice nucleators, *Phil. Trans.*
5 *R. Soc. Lond. B.*, 357, 937-943, doi:10.1098/rstb.2002.1082, 2002.

6 Morris, C. E., Sands, D. C., Vinatzer, B. A., Glaux, C., Guilbaud, C., Buffière, A., Yan, S.,
7 Dominguez, H., and Thompson, B. M.: The life history of the plant pathogen *Pseudomonas*
8 *syringae* is linked to the water cycle, *ISME Journal*, 2, 321-334, 2008.

9 Morris, C. E., Sands, D. C., Glaux, C., Samsatly, J., Asaad, S., Moukahel, A. R., Goncalves, F. I.
10 T., and Bigg, K. E.: Urediospores of rust fungi are ice nucleation active at $> -10^{\circ}\text{C}$ and harbor
11 ice nucleation active bacteria, *Atmos. Chem. Phys.*, 13, 4223-4233, 2013a.

12 Morris, C. E., Monteil, C. L., and Berge, O.: The life history of *Pseudomonas syringae*: linking
13 agriculture to Earth system processes, *Annu. Rev. Phytopathol.*, 51, 85-104, 2013b.

14 Morris, C. E., Conen, F., Huffman, J. A., Phillips, V., Pöschl, U., and Sands, D. C.:
15 Bioprecipitation: A feedback cycle linking Earth history, ecosystem dynamics and land use
16 through biological ice nucleators in the atmosphere, *Global Change Biol.*, 20, 341-351, 2014.

17 Murray, B. J., O'Sullivan, D., Atkinson, J. D., Webb, M. E.: Ice nucleation by particles immersed
18 in supercooled cloud droplets, *Chem. Soc. Rev.*, 41, 6519-6554, 2012.

19 Osborne, T.B.: Die Pflanzenproteine, *Ergebnisse der Physiologie*, 10, 47-215, 1910. (in German)

20 Schnell, R., and Vali, G.: Biogenic ice nuclei part I: Terrestrial and marine sources, *J. Atmos.*
21 *Sci.*, 33, 1554-1564, 1976.

22 Shen J. H., Klier, K., and Zettlemyer A. C.: Ice nucleation by micas, *J. Atmos. Sci.*, 34, 957-
23 960, 1977.

24 Staudinger, H., and Staudinger, M.: Die makromolekulare Chemie und ihre Bedeutung für die
25 Protoplasmaforschung; in *Protoplasmatologia*, 1, 1, 2-6, Springer-Verlag Wien GmbH,
26 doi:10.1007/978-3-7091-2448-2, 1954.

27 Steele, R.L., and Krebs, F.W.: Characteristics of silver iodide ice nuclei origination from
28 anhydrous ammonia-silver iodide complexes, part I, *J. Appl. Meteorol.*, 6.1, 1966.

1 Wallnoefer, H. G., Handschuh, S., Liedl, K. R., and Fox, T.: Stabilizing of a globular protein by a
2 highly complex water network: a molecular dynamics simulation study on factor Xa, *J. Phys.*
3 *Chem. B*, 114, 7405-7412, doi:10.1021/jp101654g, 2010.

4 Wex, H., DeMott, P. J., Tobo, Y., Hartmann, S., Rösch, M., Clauss, T., Tomsche, L., Niedermeier,
5 D., and Stratmann, F.: Kaolinite particles as ice nuclei: learning from the use of different
6 kaolinite samples and different coatings, *Atmos. Chem. Phys.*, 14, 5529-5546, doi:10.5194/acp-
7 14-5529-2014, 2014.

8 Wiacek, A., Peter, T., and Lohmann, U.: The potential influence of Asian and African mineral
9 dust on ice, mixed-phase and liquid water clouds, *Atmos. Chem. Phys.*, 10, 8649-8667,
10 doi:10.5194/acp-10-8649-2010, 2010.

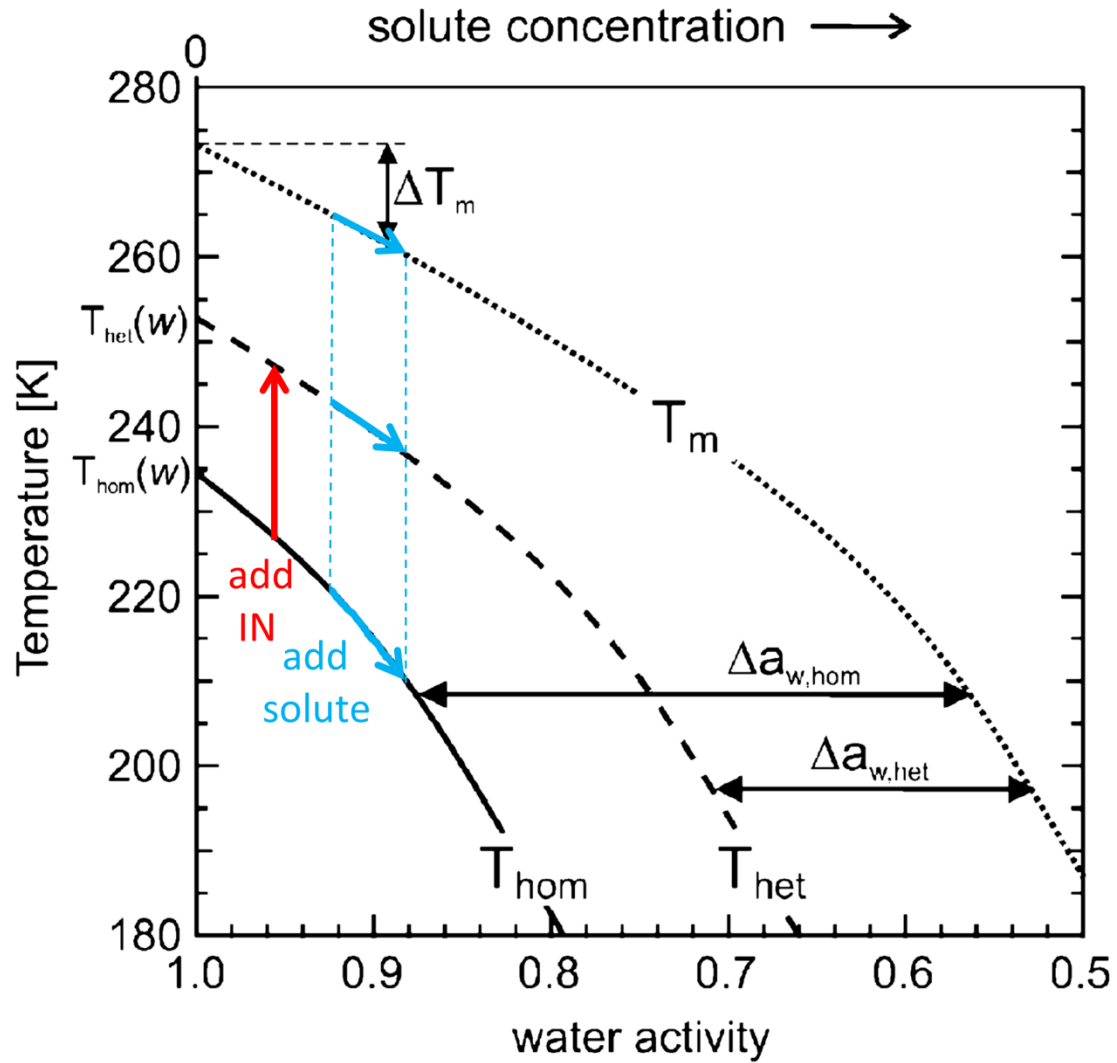
11 Zachariassen, K. E., and Kristiansen, E.: Ice nucleation and antinucleation in nature, *Cryobiol.*,
12 41, 257-279, 2000.

13 Zobrist, B., Marcolli, C., Peter, T., and Koop, T.: Heterogeneous ice nucleation in aqueous
14 solutions: the role of water activity, *J. Phys. Chem. A*, 112, 3965-3975, 2008.

15 Zolles, T., Burkart, J., Häusler, T., Pummer, B., Hitzenberger, R., and Grothe, H.: Identification
16 of ice nucleation active sites on feldspar dust particles, *J. Phys. Chem. A*, *accepted*,
17 doi:10.1021/jp509839x, 2015.

Elution time [min]	Mass range [kDa]
2.8–3.5	335–860
3.5–4.5	50–335
4.5–5.2	13–50
5.2–6.0	5–13
6.0–7.5	<5

1 Table S1: Sample fractions collected for INA tests and corresponding approximate molecular
2 weights as estimated by calibration with standards. Although all fractions contained INMs,
3 the first fraction contained the highest number concentration.



1
 2 Figure S1: Correlation between a_w and T , based on Koop and Zobrist (2009). The vectors show
 3 the impact of INs (red) and freezing point depressing solutes (blue).